Acta Crystallographica Section A
Foundations of Crystallography
ISSN 0108-7673

Received 10 July 2007
Accepted 26 September 2007

The crystallographic fast Fourier transform. Recursive symmetry reduction

Andrzej Kudlicki,‡ Maga Rowicka‡ and Zbyszek Otwinowski*

Department of Biochemistry, UT Southwestern Medical Center at Dallas, 5323 Harry Hines Boulevard, Dallas, TX 75390-8816, USA. Correspondence e-mail: zo@work.swmed.edu

Algorithms are presented for maximally efficient computation of the crystallographic fast Fourier transform (FFT). The approach is applicable to all 230 space groups and allows reduction of both the computation time and the memory usage by a factor equal to the number of symmetry operators. The central idea is a recursive reduction of the problem to a series of transforms on grids with no special points. The maximally efficient FFT for such grids has been described in previous papers by the same authors. The interaction between the grid size factorization and the symmetry operators and its influence on the algorithm design are discussed.

1. Introduction

So far, no algorithm has been found that provides efficient computation of the Fourier transform in the presence of crystallographic symmetry for most of the 230 symmetry groups. Such algorithms should operate only on the asymmetric unit and their speed should be similar to a *P*1 fast Fourier transform (FFT) of the same amount of data. Ten Eyck (1973) has presented a partial solution to this problem, working for several space groups.

Subsequently, optimization of crystallographic FFT has attracted lots of attention and has been the subject of more than 20 publications. In particular, a general approach has been proposed by Bricogne (1993), but without a prescription of how to design algorithms for a large number of space groups. All FFT implementations in today's crystallographic software are either based on Ten Eyck's ideas (Brunger, 1988; Pavelčík, 2002) or neglect the symmetry and perform the FFT on the whole unit cell.

This paper is the final in a series of articles describing our algorithms for evaluation of the crystallographic FFT. Up to now, we have presented explicit schemes for one-step symmetry reduction for 67 space groups in papers I and II (Rowicka *et al.*, 2002, 2003*a*). Then, in paper III (Rowicka *et al.*, 2003*b*), we extended this scheme by the 44 space groups containing centering translations. In paper IV (Kudlicki *et al.*, 2004), we discussed the shapes of asymmetric units in the reciprocal space. Here we present a generalized approach, based on recursive decomposition of symmetry-invariant computational grids. We show that the algorithms presented are applicable to all of the remaining symmetry groups, thus completing the theoretical foundation of maximally efficient crystallographic FFT's.

Our goal is to compute the discrete Fourier transform of a periodic function f defined on $\mathbb{Z}^3$. Such a function will have the periodicity of the underlying crystal structure. The crystal periodicity can be described by a 3×3 matrix with integer entries, $\mathbf{A}$, whose columns are the primitive translation vectors. These vectors are linearly independent, hence $\det\mathbf{A}\neq 0$. The crystal periodicity condition reads $f(\mathbf{x}+\mathbf{t})=f(\mathbf{x})$, where $\mathbf{x}\in\mathbb{Z}^3$ and $\mathbf{t}\in\mathbf{A}\mathbb{Z}^3=\{\mathbf{v}\in\mathbb{Z}^3:$ there exists $y\in\mathbb{Z}^3$ such that $\mathbf{v}=\mathbf{A}\mathbf{y}\}$. The *equivalence class* of $\mathbf{x}$ (with respect to the equivalence relation of having the same crystallographic coordinates) is defined by $[\mathbf{x}]_{\mathbf{A}}=\{\mathbf{y}\in\mathbb{Z}^3:\mathbf{y}-\mathbf{x}\in\mathbf{A}\mathbb{Z}^3\}$.

To describe the periodicity conditions in a convenient way, we shall consider the *quotient space* of $\mathbb{Z}^3$ by $\mathbf{A}\mathbb{Z}^3$ (paper II; Bricogne, 1993): $\mathbb{Z}^3/\mathbf{A}\mathbb{Z}^3=\{[\mathbf{x}]_{\mathbf{A}}:\mathbf{x}\in\mathbb{Z}^3\}$. Instead of viewing f as a periodic function, it can be considered as defined on the set of the equivalence classes, $\mathbb{Z}^3/\mathbf{A}\mathbb{Z}^3$. Let us introduce the notation

$$\Gamma=\mathbb{Z}^3/\mathbf{A}\mathbb{Z}^3 \quad\text{and}\quad \Gamma^*=\mathbb{Z}^3/\mathbf{A}^T\mathbb{Z}^3, \tag{1}$$

where $\mathbf{A}^T$ denotes the transposition of matrix $\mathbf{A}$. The space Γ^* is a space dual to Γ. Its elements are covectors, *i.e.* objects dual to vectors (Rowicka *et al.*, 2004). When there is no risk of confusion, they will be called vectors. The scalar product of a covector $\mathbf{h}\in\Gamma^*$ and a vector $\mathbf{x}\in\Gamma$ will be denoted by $\mathbf{h}\cdot\mathbf{x}$. We shall use a shorthand notation $e_{\mathbf{A}}(\mathbf{h},\mathbf{x})$ for the coefficient ('twiddle factor')

$$e_{\mathbf{A}}(\mathbf{h},\mathbf{x})=\exp(-2\pi i\mathbf{h}\cdot\mathbf{A}^{-1}\mathbf{x}).$$

Let f be a complex-valued function on Γ. The Fourier transform of f, denoted by F, is defined for $\mathbf{h}\in\Gamma^*$ by

$$F(\mathbf{h})=\sum_{\mathbf{x}\in\Gamma}f(\mathbf{x})e_{\mathbf{A}}(\mathbf{h},\mathbf{x}).$$

Assume that $\mathbf{A}_0$ and $\mathbf{A}_1$ are matrices with integer entries, such that

‡ These authors have contributed equally.

$$\mathbf{A} = \mathbf{A}_0\mathbf{A}_1. \quad (2)$$

Let us define $X_0 = \mathbb{Z}^3/\mathbf{A}_0\mathbb{Z}^3$ and $X_1 = \mathbb{Z}^3/\mathbf{A}_1\mathbb{Z}^3$. Then every element $\mathbf{x} \in \Gamma$ can be expressed uniquely as

$$\mathbf{x} = \mathbf{x}_0 + \mathbf{A}_0\mathbf{x}_1, \quad (3)$$

where $\mathbf{x}_0 \in X_0$ and $\mathbf{x}_1 \in X_1$. Analogously, we define $X_0^* = \mathbb{Z}^3/\mathbf{A}_0^T\mathbb{Z}^3$ and $X_1^* = \mathbb{Z}^3/\mathbf{A}_1^T\mathbb{Z}^3$. Then, in the reciprocal space, there is a similar unique representation for every $\mathbf{h} \in \Gamma^*$:

$$\mathbf{h} = \mathbf{h}_1 + \mathbf{A}_1^T\mathbf{h}_0, \quad (4)$$

where $\mathbf{h}_0 \in X_0^*$ and $\mathbf{h}_1 \in X_1^*$.

We will perform all the computations in the *grid coordinate system*. It is defined by the matrix $\mathbf{A}$, describing the grid Γ [equation (1)], and by a translation vector $\mathbf{b}$. Let $\mathbf{x}^c$ and $\mathbf{x}$ denote the coordinates of the same point in the crystallographic and grid coordinate systems, respectively. The transformation from the crystallographic to the grid coordinates is then given by

$$\mathbf{x} = \mathbf{A}\mathbf{x}^c + \mathbf{b}. \quad (5)$$

The relationship between the symmetry operator in the crystallographic coordinate system $(\mathbf{R}_g^c, \mathbf{t}_g^c)$ and in the grid coordinate system $(\mathbf{R}_g, \mathbf{t}_g)$ is

$$\mathbf{R}_g = \mathbf{R}_g^c \quad \text{and} \quad \mathbf{t}_g = (\mathbf{I} - \mathbf{R}_g^c)\mathbf{b} + \mathbf{A}\mathbf{t}_g^c, \quad (6)$$

where $\mathbf{I}$ is the identity matrix. Let G denote the quotient (or factor) crystallographic space group (Bricogne, 1993; paper II). The elements of G are the symmetry operators as listed in *International Tables for Crystallography* (ITC) (Hahn, 1995). The group operation in G is the ordinary composition of symmetry operators. An element $g \in G$ acts on equivalence classes $[\mathbf{x}]_\mathbf{A} = \mathbf{x} \in \Gamma = \mathbb{Z}^3/\mathbf{A}\mathbb{Z}^3$ (real space) by

$$S_g(\mathbf{x}) = \mathbf{R}_g\mathbf{x} + \mathbf{t}_g. \quad (7)$$

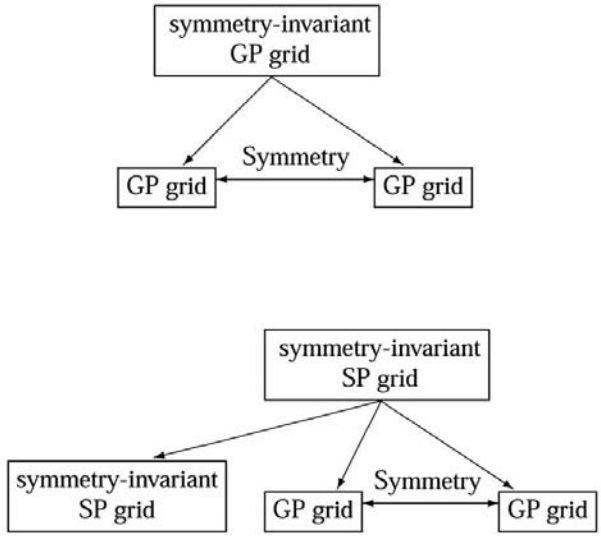

Figure 1
Differences between the decomposition employed in papers I–III (top) and in this paper (bottom). The number of SP and GP grids may vary.

The rotational part $\mathbf{R}_g$ of the symmetry operator S_g can be either a proper ($\det \mathbf{R}_g = 1$) or an improper ($\det \mathbf{R}_g = -1$) rotation. The action (7) extends to the action S^* on the Fourier transforms in the reciprocal space:

$$S_g^*F(\mathbf{h}) = e_\mathbf{A}(\mathbf{h}, \mathbf{t}_g)F(\mathbf{R}_g^T\mathbf{h}). \quad (8)$$

2. Recursive symmetry reduction

A starting point to any crystallographic FFT calculation is a symmetry-invariant periodic grid. In the cases discussed in papers I–III, we designed the maximally efficient crystallographic FFT (Appendix *A*) by employing a set of mutually disjoint symmetry-related periodic subgrids that sum up to the starting grid (Fig. 1, top). A necessary condition for such a decomposition to exist is that there are no symmetry-invariant data points; all grid points are in general positions. We will call such a grid a *GP grid*.

In this paper, we discuss efficient crystallographic FFT's when a GP grid does not exist.

A crucial observation on which this paper is based is that every grid containing points in special positions (*SP grid*) can be decomposed into a sum of disjoint periodic SP and GP grids. Moreover, one can choose symmetry-invariant SP subgrid(s) and symmetry-related GP subgrids (Fig. 1, bottom). The algorithms for symmetry-related GP grids are described in papers I–III. The SP grid(s) can be decomposed again and again until one-point grids are reached (Fig. 2). Points in special positions are computationally inconvenient, because they are different from points in general positions, and we are forced to keep track of these differences during computations.

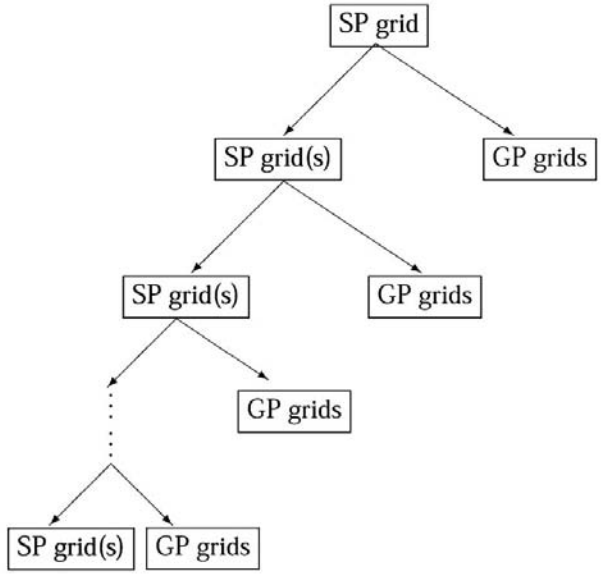

Figure 2
Recursive symmetry decomposition. Only the SP grids are decomposed further (until single-point grids are reached). The number of subgrids at every step depends on the symmetry operators and on the prime-factor decomposition of the grid size.

However, at the level of 1-point grids, the Fourier transform is trivial and a special point does not pose a problem.

The recursive symmetry decomposition is the central point of this paper and will be described in detail. This type of decomposition was studied in the one-dimensional case by Swarztrauber (1986) and mentioned in the discussion of the effects of symmetry on the Cooley–Tukey decomposition by Bricogne (1993).

3. Diagonal mirror symmetry

We begin presentation of recursive symmetry decomposition with a simple case of the 'diagonal mirror' crystallographic symmetry (symmetry operator y, x, z). We consider the two-dimensional case because the symmetry in the third dimension is trivial. Let us assume for a moment that the grid size is divisible by two. Now the crystal periodicity can be described by the matrix $\mathbf{A}$:

$$\mathbf{A} = \begin{bmatrix} 2N & 0 \\ 0 & 2N \end{bmatrix},$$

where N is an integer and $\det \mathbf{A}$ equals the number of grid points in the two-dimensional unit cell. By (6), the diagonal mirror symmetry description is the same in both the grid and the crystallographic coordinates ($\mathbf{b} = -\frac{1}{2}\mathbf{e}_1 - \frac{1}{2}\mathbf{e}_2$, where $\mathbf{e}_1, \mathbf{e}_2$ are standard basis vectors of $\mathbb{Z}^2$):

$$\mathbf{R}_\alpha = \begin{bmatrix} 0 & 1 \\ 1 & 0 \end{bmatrix}, \quad \mathbf{t}_\alpha = \begin{bmatrix} 0 \\ 0 \end{bmatrix}.$$

Let us choose the matrices $\mathbf{A}_0$ and $\mathbf{A}_1$, describing the decomposition of $\Gamma = \mathbb{Z}^2/\mathbf{A}\mathbb{Z}^2$ given by (2), as:

$$\mathbf{A}_0 = \begin{bmatrix} 2 & 0 \\ 0 & 2 \end{bmatrix} \quad \text{and} \quad \mathbf{A}_1 = \begin{bmatrix} N & 0 \\ 0 & N \end{bmatrix}.$$

In other words, we decompose Γ into four subgrids, according to the parity of the x and y coordinates, *i.e.* the first grid $\Gamma_0 = \mathbf{A}_0 X_1$ (colored red in Fig. 3) has both coordinates even *etc*. We use the decomposition of $\mathbf{x}$, given by (3), to introduce four new functions:

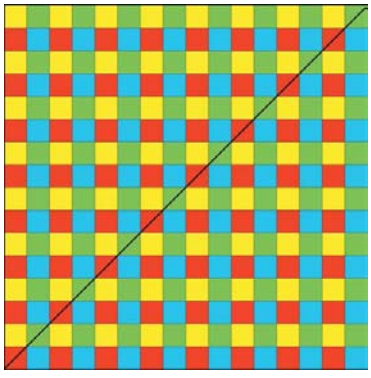

Figure 3
Subgrid decomposition for the diagonal mirror symmetry. The data points are located in the centers of the colored squares. There are two SP subgrids red (Γ_0) and green and two GP ones (blue and yellow).

$$\left.\begin{aligned} f_{00}(\mathbf{x}_1) &= f(\mathbf{A}_0\mathbf{x}_1) \\ f_{10}(\mathbf{x}_1) &= f(\mathbf{A}_0\mathbf{x}_1 + \mathbf{e}_1) \\ f_{01}(\mathbf{x}_1) &= f(\mathbf{A}_0\mathbf{x}_1 + \mathbf{e}_2) \\ f_{11}(\mathbf{x}_1) &= f(\mathbf{A}_0\mathbf{x}_1 + \mathbf{e}_1 + \mathbf{e}_2), \end{aligned}\right\} \tag{9}$$

where $\mathbf{x}_1 \in X_1 = \mathbb{Z}^2/\mathbf{A}_1\mathbb{Z}^2$. Then, the Fourier transform F can be expressed as a combination of transforms of the four functions defined above:

$$\begin{aligned} F(\mathbf{h}) &= \sum_{\mathbf{x}\in\Gamma} f(\mathbf{x}) e_{\mathbf{A}}(\mathbf{h}, \mathbf{x}) \\ &= \sum_{\mathbf{x}\in\Gamma_0} f(\mathbf{x}) e_{\mathbf{A}}(\mathbf{h}, \mathbf{x}) + \sum_{\mathbf{x}\in\Gamma_0} f(\mathbf{x}+\mathbf{e}_1) e_{\mathbf{A}}(\mathbf{h}, \mathbf{x}+\mathbf{e}_1) \\ &\quad + \sum_{\mathbf{x}\in\Gamma_0} f(\mathbf{x}+\mathbf{e}_2) e_{\mathbf{A}}(\mathbf{h}, \mathbf{x}+\mathbf{e}_2) \\ &\quad + \sum_{\mathbf{x}\in\Gamma_0} f(\mathbf{x}+\mathbf{e}_1+\mathbf{e}_2) e_{\mathbf{A}}(\mathbf{h}, \mathbf{x}+\mathbf{e}_1+\mathbf{e}_2) \\ &= \sum_{\mathbf{x}_1\in X_1} f_{00}(\mathbf{x}_1) e_{\mathbf{A}_1}(\mathbf{h}, \mathbf{x}_1) + e_{\mathbf{A}}(\mathbf{h}, \mathbf{e}_1) \sum_{\mathbf{x}_1\in X_1} f_{10}(\mathbf{x}_1) e_{\mathbf{A}_1}(\mathbf{h}, \mathbf{x}_1) \\ &\quad + e_{\mathbf{A}}(\mathbf{h}, \mathbf{e}_2) \sum_{\mathbf{x}_1\in X_1} f_{01}(\mathbf{x}_1) e_{\mathbf{A}_1}(\mathbf{h}, \mathbf{x}_1) \\ &\quad + e_{\mathbf{A}}(\mathbf{h}, \mathbf{e}_1+\mathbf{e}_2) \sum_{\mathbf{x}_1\in X_1} f_{11}(\mathbf{x}_1) e_{\mathbf{A}_1}(\mathbf{h}, \mathbf{x}_1). \end{aligned}$$

Let us now use the decomposition of $\mathbf{h}$, given by (4). It follows that

$$e_{\mathbf{A}_1}(\mathbf{h}, \mathbf{x}_1) = e_{\mathbf{A}_1}(\mathbf{h}_1 + \mathbf{A}_1^T\mathbf{h}_0, \mathbf{x}_1) = e_{\mathbf{A}_1}(\mathbf{h}_1, \mathbf{x}_1), \tag{10}$$

because both $\mathbf{h}_0$ and $\mathbf{x}_1$ have integer components

$$\begin{aligned} e_{\mathbf{A}_1}(\mathbf{A}_1^T\mathbf{h}_0, \mathbf{x}_1) &= e_{\mathbf{A}_1}(\mathbf{h}_0, \mathbf{A}_1\mathbf{x}_1) \\ &= \exp(-2\pi i \mathbf{h}_0 \cdot (\mathbf{A}_1)^{-1}\mathbf{A}_1\mathbf{x}_1) = 1. \end{aligned}$$

We will use this simple observation repeatedly later on. Let F_{00} denote the Fourier transform of the function f_{00}:

$$F_{00}(\mathbf{h}_1) = \sum_{\mathbf{x}_1\in X_1} f_{00}(\mathbf{x}_1) e_{\mathbf{A}_1}(\mathbf{h}_1, \mathbf{x}_1),$$

where $\mathbf{h}_1 \in \mathbb{Z}^2/\mathbf{A}_1^T\mathbb{Z}^2$. Analogously, let F_{01}, F_{10} and F_{11} denote the Fourier transforms of the functions f_{01}, f_{10} and f_{11}, respectively. Then, by (10),

$$\begin{aligned} F(\mathbf{h}) &= F_{00}(\mathbf{h}_1) + e_{\mathbf{A}}(\mathbf{h}, \mathbf{e}_1) F_{10}(\mathbf{h}_1) \\ &\quad + e_{\mathbf{A}}(\mathbf{h}, \mathbf{e}_2) F_{01}(\mathbf{h}_1) + e_{\mathbf{A}}(\mathbf{h}, \mathbf{e}_1+\mathbf{e}_2) F_{11}(\mathbf{h}_1). \end{aligned} \tag{11}$$

Since $f(\mathbf{x}) = f(\mathbf{R}_\alpha\mathbf{x})$ and $\mathbf{R}_\alpha^2 = \mathbf{I}$, it follows that

$$\begin{aligned} e_{\mathbf{A}}(\mathbf{h}, \mathbf{e}_1) F_{10}(\mathbf{h}_1) &= \sum_{\mathbf{x}\in\Gamma_0} f(\mathbf{x}+\mathbf{e}_1) e_{\mathbf{A}}(\mathbf{h}, \mathbf{x}+\mathbf{e}_1) \\ &= \sum_{\mathbf{x}\in\Gamma_0} f(\mathbf{R}_\alpha(\mathbf{x}+\mathbf{e}_1)) e_{\mathbf{A}}(\mathbf{R}_\alpha^T\mathbf{h}, \mathbf{R}_\alpha(\mathbf{x}+\mathbf{e}_1)) \\ &= \sum_{\mathbf{x}\in\Gamma_0} f(\mathbf{R}_\alpha\mathbf{x}+\mathbf{e}_2) e_{\mathbf{A}}(\mathbf{R}_\alpha^T\mathbf{h}, (\mathbf{R}_\alpha\mathbf{x}+\mathbf{e}_2)) \\ &= e_{\mathbf{A}}(\mathbf{R}_\alpha^T\mathbf{h}, \mathbf{e}_2) F_{01}(\mathbf{R}_\alpha^T\mathbf{h}_1). \end{aligned}$$

Moreover,

$$e_{\mathbf{A}}(\mathbf{R}_\alpha^T\mathbf{h}, \mathbf{e}_2) = e_{\mathbf{A}}(\mathbf{h}, \mathbf{R}_\alpha\mathbf{e}_2) = e_{\mathbf{A}}(\mathbf{h}, \mathbf{e}_1).$$

After substituting the thus derived relationship,

$$F_{10}(\mathbf{h}_1) = F_{01}(\mathbf{R}_\alpha^T\mathbf{h}_1), \tag{12}$$

into (11), we obtain

$$F(\mathbf{h}) = F_{00}(\mathbf{h}_1) + e_{\mathbf{A}}(\mathbf{h}, \mathbf{e}_1 + \mathbf{e}_2)F_{11}(\mathbf{h}_1) + e_{\mathbf{A}}(\mathbf{h}, \mathbf{e}_1)F_{01}(\mathbf{R}_\alpha^T\mathbf{h}_1) + e_{\mathbf{A}}(\mathbf{h}, \mathbf{e}_2)F_{01}(\mathbf{h}_1). \quad (13)$$

The Fourier transform F of the entire unit cell can be expressed by the three transforms F_{00}, F_{11} and F_{01} [equation (13)]. Thus the computation of the Fourier transform of the initial number of points is reduced to the computation of three Fourier transforms each of one quarter of all points. The transform F_{01} has no internal symmetry, therefore it will be calculated directly. The two transforms F_{00} and F_{11} reveal diagonal mirror symmetry, therefore they can be decomposed again, by applying equation (13) with F_{00} or F_{11} substituted as the new F.

If N is a power of 2, we can repeat this decomposition until we reach one-point grids. The resulting asymmetric unit consists of several regular subgrids of different sizes and has a self-similar fractal-like shape (Fig. 4).

At the first step of the decomposition, one GP grid of N^2 points is added to the asymmetric unit. In the next step, we add one GP grid of $N^2/4$ points for each of the two N^2-point GP grids and so on until the last step, when we add $3N$ 1-point grids to the asymmetric unit. From these, N are GP and $2N$ are SP grids ($2N$ is the number of grid points along the diagonal). Therefore, the size of the thus chosen asymmetric unit can be computed as

$$\left\{N^2 + \frac{N^2}{2} + \frac{N^2}{2^2} + \ldots + \frac{N^2}{2^{n-1}} + \frac{N^2}{2^n}\right\} + 2N = 2N^2 + N.$$

The total number of points in the unit cell is $4N^2$, so the fraction of unit-cell points belonging to the asymmetric unit is $\frac{1}{2} + 1/(4N)$ and converges to $\frac{1}{2}$ for large N.

Let us now switch to the general case where the number of data points is not necessarily divisible by two. Since the number of grid points is always a square of an integer, each factor in its prime-number decomposition appears twice. Suppose now that the number of grid points is p^2N^2, where p is a prime number. Then we decompose the grid Γ into p^2 subgrids according to the values of coordinates modulo p:

$$\mathbf{A} = \begin{bmatrix} pN & 0 \\ 0 & pN \end{bmatrix}, \quad \mathbf{A}_0 = \begin{bmatrix} p & 0 \\ 0 & p \end{bmatrix}, \quad \mathbf{A}_1 = \begin{bmatrix} N & 0 \\ 0 & N \end{bmatrix}.$$

For example, if $p = 3$, we divide the grid into nine subgrids. Three of these subgrids (those with both coordinates equal modulo 3) will be symmetry-invariant SP grids, and the other six will form three pairs of symmetry-related GP grids. The result we get is

$$F(\mathbf{h}) = F_{00}(\mathbf{h}_1) + e_{\mathbf{A}}(\mathbf{h}, \mathbf{e}_1)F_{10}(\mathbf{h}_1) + \sum_{q=0}^{1}\sum_{r=q+1}^{2}\left\{e_{\mathbf{A}}(\mathbf{h}, q\mathbf{e}_1 + r\mathbf{e}_2)F_{qr}(\mathbf{h}_1) + e_{\mathbf{A}}(\mathbf{h}, r\mathbf{e}_1 + q\mathbf{e}_2)F_{qr}(\mathbf{R}_\alpha^T\mathbf{h}_1)\right\}. \quad (14)$$

For a general prime factor p, we obtain p symmetry-invariant SP subgrids (again, these will be the subgrids with both coordinates equal modulo p) and $p^2 - p$ subgrids of the GP type, which will form $p(p-1)/2$ pairs of symmetry-related GP subgrids.

3.1. Diagonal glide planes

For the symmetry operator $y + \frac{1}{2}, x + \frac{1}{2}$ (ITC groups 100, 113, 125, 127, 129 and 138), the above reasoning is valid after substitution of

$$F(\mathbf{h}_1) = e_{\mathbf{A}}(\mathbf{h}, \mathbf{t}_g)F(\mathbf{R}_\alpha^T\mathbf{h}_1), \quad (15)$$

where

$$\mathbf{t}_g = \begin{bmatrix} N \\ N \end{bmatrix},$$

in place of (12).

Similar small changes (and switching to the three-dimensional space) are needed to treat glide planes related to the symmetry operators $y, x, z + \frac{1}{2}$ (ITC groups 103, 105, 112, 124, 131 and 133) and $y + \frac{1}{2}, x + \frac{1}{2}, z + \frac{1}{2}$ (ITC groups 104, 106, 114, 126, 128, 130, 135 and 137).

3.2. Combining diagonal mirror symmetry with body centering (*i.e.* with the symmetry operator $x + \frac{1}{2}, y + \frac{1}{2}, z + \frac{1}{2}$)

To combine the diagonal mirror decomposition with reduction of body centering, we assume the following form of matrix $\mathbf{A}$ and vector $\mathbf{b}$:

$$\mathbf{A} = \begin{bmatrix} 4N & 0 & 0 \\ 0 & 4N & 0 \\ 0 & 0 & 2Q \end{bmatrix} \quad \text{and} \quad \mathbf{b} = -\tfrac{1}{2}\mathbf{e}_1 - \tfrac{1}{2}\mathbf{e}_2 - \tfrac{1}{2}\mathbf{e}_3,$$

where N and Q are positive integers. The grid in the xy plane is decomposed as in the diagonal mirror case. The resulting GP grids are symmetry invariant for the operator $x + \frac{1}{2}, y + \frac{1}{2}, z + \frac{1}{2}$. Therefore, we can reduce body centering as in paper III and compute the Fourier transform on the asymmetric part. We proceed with the diagonal mirror algorithm computing the FFT at every step on GP grids after

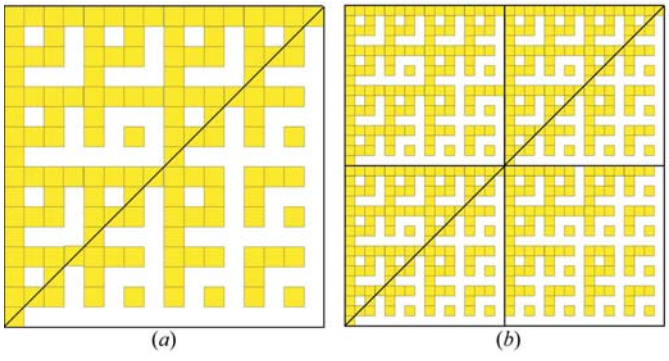

Figure 4
A fractal-like asymmetric unit for the diagonal mirror symmetry consists of several regular subgrids of different sizes. Left: 16×16 unit cell. Right: 32×32 unit cell. It contains two exact copies of the asymmetric unit for the 16×16 unit cell and two slightly altered copies. The two exact copies lie on the diagonal of the 32×32 unit cell.

reducing their body centering. This is the case of the ITC groups 107, 108, 121, 139 and 140.

If, instead of the diagonal mirror symmetry operator y, x, z we are dealing with the operator $y+\frac{1}{2}, x, z+\frac{3}{4}$ (groups 109, 122 and 141) or $y+\frac{1}{2}, x, z+\frac{1}{4}$ (groups 110 and 142), everything except the form of $\mathbf{t}_g$ in (15) remains the same.

4. Trigonal groups

We start with the basic example of the $p3$ symmetry, then proceed to $p6$ symmetry and also comment on groups such as $p3m1$ and rhombohedral centering.

4.1. $p3$ symmetry with special points

The $p3$ symmetry reduction with all points in general positions was addressed in paper I. However, as we shall see, in some cases it is necessary to reduce the $p3$ symmetry in the presence of special points. Then we will use a recursive algorithm similar to our solution for the diagonal mirror symmetry. Let assume that

$$A = \begin{bmatrix} M & 0 \\ 0 & M \end{bmatrix}$$

and that M is a positive integer. The algorithm presented works for any positive integer value of M, however we shall start with an example of even M. In this case, $M = 2N$ and

$$\mathbf{A}_0 = \begin{bmatrix} 2 & 0 \\ 0 & 2 \end{bmatrix} \quad \text{and} \quad \mathbf{A}_1 = \begin{bmatrix} N & 0 \\ 0 & N \end{bmatrix},$$

where N is a positive integer (Fig. 5).

Note that this decomposition gives one SP subgrid and three GP subgrids. The SP subgrid is invariant under the action of the $p3$ group and the three GP subgrids are transformed into each other. Therefore, it is sufficient to keep one of these GP grids in the asymmetric unit.

In the general case, we shall use a prime factor of M, p. We define N by $M = pN$ and perform the following decomposition:

$$\mathbf{A} = \begin{bmatrix} pN & 0 \\ 0 & pN \end{bmatrix}, \quad \mathbf{A}_0 = \begin{bmatrix} p & 0 \\ 0 & p \end{bmatrix}, \quad \mathbf{A}_1 = \begin{bmatrix} N & 0 \\ 0 & N \end{bmatrix}.$$

For example, if $p = 3$, then

$$\mathbf{A}_0 = \begin{bmatrix} 3 & 0 \\ 0 & 3 \end{bmatrix},$$

i.e. we divide the grid into nine subgrids. Three of these grids have points on axes and six do not. Until now, the decomposition has been the same as for diagonal mirror symmetry. However, in the case of the $p3$ symmetry, the relationship between these six GP subgrids are different. Specifically, there are two triples of symmetry-related GP grids (Fig. 6). Therefore, to know the Fourier transform of the whole grid it is sufficient to compute it on the three SP subgrids and two properly chosen (out of six) GP grids.

If $p = 5$, this decomposition yields 1 SP subgrid and 24 GP subgrids, from which we properly choose 8. Let us now consider the case of a general prime number p. For simplicity, since the case of $p = 3$ was discussed above, suppose that $p \neq 3$. Observe that we will have only one (up to primitive translations) special point in every unit cell (three for the case of $p = 3$). Therefore, it is evidently possible to decompose the original SP grid into p^2 subgrids in such a way that only one resulting subgrid is a SP subgrid (there will be three SP subgrids for $p = 3$). Thus, we will get $p^2 - 1$ symmetry-related GP subgrids. One of the three consecutive integers is always divisible by three. In our case of consecutive integers, $p-1, p, p+1$, the one divisible by three must be either $p-1$ or $p+1$ because p is assumed to be prime and not equal to three. Therefore, $p^2 - 1 = (p-1)(p+1)$ will be always divisible by three. Consequently, the $p^2 - 1$ GP grids are arranged into $(p^2-1)/3$ triples of GP grids related by the $p3$ symmetry. It is sufficient to compute the FFT on one representative of every symmetry-related triple of GP grids.

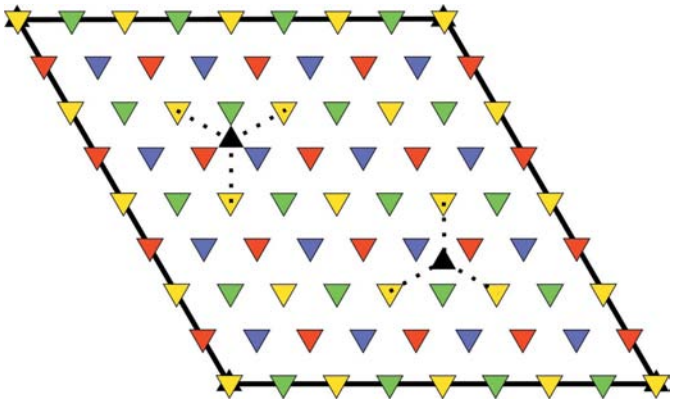

Figure 5
Subgrid decomposition for the $p3$ symmetry for even numbers of points along x and y axes. All grid points lie in the centers of colored triangles. The SP grid is yellow, the GP grids are red, blue and green. The SP grid retains the $p3$ symmetry.

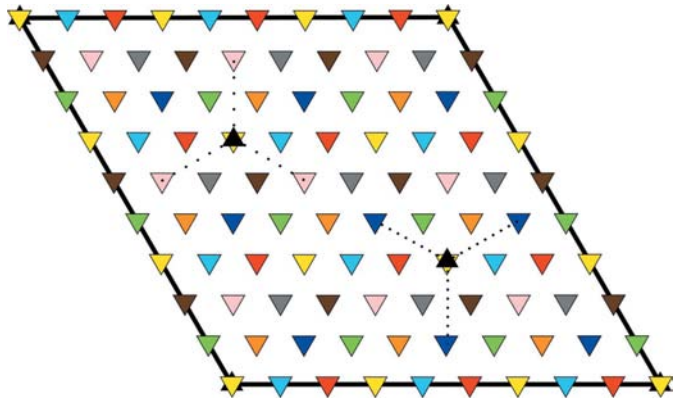

Figure 6
Subgrid decomposition for the $p3$ symmetry when the number of points along x and y axes is odd and divisible by 3. Note that all SP grids (yellow, light pink and dark blue) are $p3$ symmetry invariant. Moreover, there are two triples, (green, turquoise, grey) and (orange, red, brown), of symmetry-related GP grids.

Now we come back to the case of even N and describe it in more detail. Let

$$\mathbf{A} = \begin{bmatrix} 2N & 0 \\ 0 & 2N \end{bmatrix} \quad \text{and} \quad \mathbf{b} = \begin{bmatrix} 0 \\ 0 \end{bmatrix}$$

and let us choose

$$\mathbf{A}_0 = \begin{bmatrix} 2 & 0 \\ 0 & 2 \end{bmatrix} \quad \text{and} \quad \mathbf{A}_1 = \begin{bmatrix} N & 0 \\ 0 & N \end{bmatrix}.$$

Then,

$$\Gamma = \mathbb{Z}^2/\mathbf{A}\mathbb{Z}^2 \quad \text{and} \quad X_1 = \mathbb{Z}^2/\mathbf{A}_1\mathbb{Z}^2.$$

Let α denote the symmetry operator $\bar{y}, x - y$, which encodes the 120° counterclockwise rotation. Then, the symmetry operators α and α^2 are described in the grid coordinates by matrices

$$\mathbf{R}_\alpha = \begin{bmatrix} 0 & -1 \\ 1 & -1 \end{bmatrix} \quad \text{and} \quad \mathbf{R}_{\alpha^2} = \begin{bmatrix} -1 & 1 \\ -1 & 0 \end{bmatrix},$$

respectively. Let f be a function defined on Γ. Exactly as in the case of the diagonal mirror symmetry, we introduce four new functions: f_{00}, f_{10}, f_{01} and f_{11}, given by (9). We can also derive the decomposition formula, which has the same form as (11). Since $f(\mathbf{x}) = f(\mathbf{R}_\alpha \mathbf{x})$ and $\mathbf{R}_\alpha^3 = \mathbf{I}$, by (10), it follows that

$$\begin{aligned} F_{10}(\mathbf{h}_1) &= \sum_{\mathbf{x}\in\Gamma_0} f(\mathbf{x} + \mathbf{e}_1) e_{\mathbf{A}}(\mathbf{h}, \mathbf{x}) \\ &= \sum_{\mathbf{x}\in\Gamma_0} f(\mathbf{R}_\alpha(\mathbf{x} + \mathbf{e}_1)) e_{\mathbf{A}}(\mathbf{R}_{\alpha^2}^T \mathbf{h}, \mathbf{R}_\alpha \mathbf{x}) \\ &= \sum_{\mathbf{x}\in\Gamma_0} f(\mathbf{R}_\alpha \mathbf{x} + \mathbf{e}_2) e_{\mathbf{A}}(\mathbf{R}_{\alpha^2}^T \mathbf{h}, \mathbf{R}_\alpha \mathbf{x}) \\ &= \sum_{\mathbf{x}\in\Gamma_0} f_{01}(\mathbf{R}_\alpha \mathbf{x}) e_{\mathbf{A}}(\mathbf{R}_{\alpha^2}^T \mathbf{h}, \mathbf{R}_\alpha \mathbf{x}) \\ &= F_{01}(\mathbf{R}_{\alpha^2}^T \mathbf{h}_1). \end{aligned}$$

Therefore, in this case the symmetry of the Fourier transform is given by

$$F_{10}(\mathbf{h}_1) = F_{01}(\mathbf{R}_{\alpha^2}^T \mathbf{h}_1), \quad \text{hence} \quad F_{01}(\mathbf{h}_1) = F_{10}(\mathbf{R}_\alpha^T \mathbf{h}_1). \quad (16)$$

Note that the above expressions are different from (12). Analogously, we obtain the formula relating F_{11} to F_{10}:

$$\begin{aligned} F_{11}(\mathbf{h}_1) &= \sum_{\mathbf{x}\in\Gamma_0} f(\mathbf{x} + \mathbf{e}_1 + \mathbf{e}_2) e_{\mathbf{A}}(\mathbf{h}, \mathbf{x}) \\ &= \sum_{\mathbf{x}\in\Gamma_0} f(\mathbf{R}_\alpha(\mathbf{x} + \mathbf{e}_1 + \mathbf{e}_2)) e_{\mathbf{A}}(\mathbf{R}_{\alpha^2}^T \mathbf{h}, \mathbf{R}_\alpha \mathbf{x}) \\ &= \sum_{\mathbf{x}\in\Gamma_0} f((\mathbf{R}_\alpha \mathbf{x} - 2\mathbf{e}_1) + \mathbf{e}_1) e_{\mathbf{A}}(\mathbf{R}_{\alpha^2}^T \mathbf{h}, \mathbf{R}_\alpha \mathbf{x} - 2\mathbf{e}_1) \\ &\quad \times e_{\mathbf{A}}(\mathbf{R}_{\alpha^2}^T \mathbf{h}, 2\mathbf{e}_1) \\ &= e_{\mathbf{A}}(\mathbf{R}_{\alpha^2}^T \mathbf{h}, 2\mathbf{e}_1) F_{10}(\mathbf{R}_{\alpha^2}^T \mathbf{h}_1). \end{aligned}$$

Since $e_{\mathbf{A}}(\mathbf{R}_{\alpha^2}^T \mathbf{h}, 2\mathbf{e}_1) = e_{\mathbf{A}}(\mathbf{h}, -2\mathbf{e}_1 - 2\mathbf{e}_2)$, it follows that

$$F_{11}(\mathbf{h}_1) = e_{\mathbf{A}}(\mathbf{h}, -2\mathbf{e}_1 - 2\mathbf{e}_2) F_{10}(\mathbf{R}_{\alpha^2}^T \mathbf{h}_1). \quad (17)$$

Therefore, after substituting (16) and (17) into formula (11) and simplifying coefficients, we obtain

$$\begin{aligned} F(\mathbf{h}) = F_{00}(\mathbf{h}_1) &+ e_{\mathbf{A}}(\mathbf{h}, \mathbf{e}_1) F_{10}(\mathbf{h}_1) + e_{\mathbf{A}}(\mathbf{h}, \mathbf{e}_2) F_{10}(\mathbf{R}_\alpha^T \mathbf{h}_1) \\ &+ e_{\mathbf{A}}(\mathbf{h}, -\mathbf{e}_1 - \mathbf{e}_2) F_{10}(\mathbf{R}_{\alpha^2}^T \mathbf{h}_1). \end{aligned} \quad (18)$$

The above formula shows that in order to compute the Fourier transform F it is sufficient to compute the Fourier transform F_{10} on $\frac{1}{4}$ of the data points and apply a similar (depending on factorization of N) decomposition to compute the Fourier transform F_{00}.

Let us assume for a moment that $N = 2^n$. Then, in order to reduce the symmetry further, the SP grid should be divided into four subgrids again, and so on, as in the diagonal mirror case. The asymmetric unit (on which we will compute the Fourier transform) should consist of one GP grid from every stage of decomposition plus all 1-point SP grids. Observe that at the first step of the decomposition one GP grid of N^2 points is added to the asymmetric unit. In the next step, we add one GP grid of $N^2/4$ points, and so on, until the last step, when we add one 1-point GP grid to the asymmetric unit. Moreover, in this last step, we also add the only 1-point SP grid generated during this decomposition. Therefore, the size of the thus chosen asymmetric unit can be computed as follows (keeping in mind the assumption that $N^2 = 4^n$):

$$\left\{N^2 + \frac{N^2}{4} + \frac{N^2}{4^2} + \ldots + \frac{N^2}{4^n}\right\} + 1 = \frac{4N^2 - 1}{3} + 1 = \frac{4N^2 + 2}{3}.$$

In other words, the size of the asymmetric unit is the smallest integer greater than $4N^2/3$, *i.e.* the smallest possible asymmetric unit. If N is not a power of two, then we decompose our grid consecutively according to the prime-factor decomposition of N analogously to the diagonal mirror case. The difference is the relative number of SP and GP grids and symmetry relations of the latter, as discussed above.

4.2. The *p*6 symmetry

The factor crystallographic group corresponding to the $p3$ symmetry is $\{e, \alpha, \alpha^2\}$, with the notation from the previous subsection. This group is a subgroup of the factor crystallographic group corresponding to the $p6$ symmetry. This group, G, consists of the following elements:

$$G = \{e, \alpha, \alpha^2, \beta, \alpha\beta, \alpha^2\beta\},$$

where β denotes the 180° rotation operator $\bar{x}, \bar{y}, z$:

$$\mathbf{R}_\beta = \begin{bmatrix} -1 & 0 \\ 0 & -1 \end{bmatrix}.$$

Let us assume that the $p3$ symmetry induced by the subgroup $\{e, \alpha, \alpha^2\}$ is reduced in the same way as in the previous section. The β-invariance properties of the subgrids obtained during reduction of the $p3$ symmetry depend on the form of the matrices $\mathbf{A}$ and $\mathbf{A}_0$. Therefore, before we proceed to reducing the residual twofold symmetry induced by β, we have to know the form of these matrices. Let us assume that $\mathbf{A}_0 = 2\mathbf{I}$ and that the initial number of grid points was not divisible by three. Then all subgrids obtained during $p3$ symmetry reduction are invariant with respect to the 180° rotation. Therefore, we can choose any of the GP grids with respect to the $p3$ symmetry and reduce the symmetry induced by the 180° rotation.

However, if $\mathbf{A}_0 = p\mathbf{I}$, where p is prime and different from two or three,[1] then the only β-invariant subgrid will be the SP subgrid on which f_{00} is defined. Therefore, instead of decomposing any of these subgrids further, it will be sufficient to identify pairs of GP subgrids that are related through a 180° rotation, and keep only one representative of each pair in the asymmetric unit. (Note that grids in these pairs are not related by a 120° rotation.) Namely, instead of $(p^2-1)/3$ GP subgrids, it is sufficient to add to the asymmetric unit at the first step only $(p^2-1)/6$ of them, chosen in such a way that they are related neither through $p3$ symmetry nor through a 180° rotation. [Note that since p is prime then p^2-1 is even if $p \neq 2$. Moreover, as explained in the previous subsection, $p^2-1=(p-1)(p+1)$ is divisible by three if $p \neq 3$. Therefore, for $p \neq 2$ and $p \neq 3$, the expression p^2-1 is divisible by six and the number $(p^2-1)/6$ is integer.]

Let us now focus on the case when $\mathbf{A} = 2N\mathbf{I}$ and $\mathbf{A}_0 = 2\mathbf{I}$. Then the formulae (11) and (18) can be applied. Our starting grid for the reduction of symmetry induced by β will be the one on which the function f_{10} is defined [equation (9)], that is the grid whose elements are of the form $\mathbf{A}_0\mathbf{x}_1 + \mathbf{e}_1$. We begin reducing the twofold symmetry by checking whether there are special points with respect to this symmetry. A necessary condition for a point to be invariant with respect to the symmetry operator in question is that

$$\mathbf{R}_\beta(\mathbf{A}_0\mathbf{x}_1 + \mathbf{e}_1) = \mathbf{A}_0\mathbf{x}_1 + \mathbf{e}_1.$$

One can check that $\mathbf{R}_\beta$ commutes with $\mathbf{A}_0$. It follows that

$$\begin{aligned}\mathbf{R}_\beta(\mathbf{A}_0\mathbf{x}_1 + \mathbf{e}_1) &= \mathbf{R}_\beta\mathbf{A}_0\mathbf{x}_1 + \mathbf{R}_\beta\mathbf{e}_1\\ &= \mathbf{A}_0\mathbf{R}_\beta\mathbf{x}_1 - \mathbf{e}_1\\ &= \mathbf{A}_0\mathbf{R}_\beta\mathbf{x}_1 - 2\mathbf{e}_1 + \mathbf{e}_1\\ &= \mathbf{A}_0(\mathbf{R}_\beta\mathbf{x}_1 - \mathbf{e}_1) + \mathbf{e}_1.\end{aligned}$$

Therefore, the coordinates of the symmetry-invariant point have to satisfy the condition

$$\mathbf{x}_1 = \mathbf{R}_\beta\mathbf{x}_1 - \mathbf{e}_1.$$

Since the matrix describing our computational grid is now $\mathbf{A}_1 = N\mathbf{I}$, it follows that the x and y coordinates should be understood modulo N. Therefore, the solution of the above invariance condition is either $(x=(N-1)/2,\ y=N/2)$ or $(x=(N-1)/2,\ y=0)$. Hence, since grid coordinates of data points are integer, there are no fixed grid points, provided that N is even. Let us assume for a moment that this is the case, *i.e.* that N is divisible by 2. Then, we can define

$$\tilde{\mathbf{A}}_0 = \begin{bmatrix}2 & 0\\ 0 & 1\end{bmatrix} \quad \text{and} \quad \tilde{\mathbf{A}}_1 = \begin{bmatrix}\frac{N}{2} & 0\\ 0 & N\end{bmatrix}.$$

Note that

$$\mathbf{A}_1 = \tilde{\mathbf{A}}_0\tilde{\mathbf{A}}_1 \quad \text{and} \quad \mathbf{A} = \mathbf{A}_0\tilde{\mathbf{A}}_0\tilde{\mathbf{A}}_1.$$

We will decompose $\mathbf{x}_1$ again, according to (3):

$$\mathbf{x}_1 = \tilde{\mathbf{A}}_0\tilde{\mathbf{x}}_1 + \tilde{\mathbf{x}}_0,$$

where $\tilde{\mathbf{x}}_1 \in \tilde{X}_1 = \mathbb{Z}^2/\tilde{\mathbf{A}}_1\mathbb{Z}^2$ and $\tilde{\mathbf{x}}_0 \in \tilde{X}_0 = \mathbb{Z}^2/\tilde{\mathbf{A}}_0\mathbb{Z}^2 = \{\mathbf{0}, \mathbf{e}_1\}$. Let us also define

$$\begin{aligned}f_{10,0}(\tilde{\mathbf{x}}_1) &= f_{10}(\tilde{\mathbf{A}}_0\tilde{\mathbf{x}}_1) = f(\mathbf{A}_0\tilde{\mathbf{A}}_0\tilde{\mathbf{x}}_1 + \mathbf{e}_1)\\ f_{10,1}(\tilde{\mathbf{x}}_1) &= f_{10}(\tilde{\mathbf{A}}_0\tilde{\mathbf{x}}_1 + \mathbf{e}_1) = f(\mathbf{A}_0(\tilde{\mathbf{A}}_0\tilde{\mathbf{x}}_1 + \mathbf{e}_1) + \mathbf{e}_1).\end{aligned}$$

Let $F_{10,0}$ and $F_{10,1}$ denote the Fourier transforms of the functions $f_{10,0}$ and $f_{10,1}$, respectively. Analogously to the decomposition of $\mathbf{x}_1$, we have the following decomposition of $\mathbf{h}_1$:

$$\mathbf{h}_1 = \tilde{\mathbf{h}}_1 + \tilde{\mathbf{A}}_1^T\tilde{\mathbf{h}}_0,$$

where $\tilde{\mathbf{h}}_1 \in \mathbb{Z}^2/\tilde{\mathbf{A}}_1^T\mathbb{Z}^2$ and $\tilde{\mathbf{h}}_0 \in \mathbb{Z}^2/\tilde{\mathbf{A}}_0^T\mathbb{Z}^2 = \{\mathbf{0}, \mathbf{e}_1^*\}$. That is,

$$F_{10,0}(\tilde{\mathbf{h}}_1) = \sum_{\tilde{\mathbf{x}}_1\in\tilde{X}_1} f_{10,0}(\tilde{\mathbf{x}}_1)e_{\tilde{\mathbf{A}}_1}(\tilde{\mathbf{h}}_1, \tilde{\mathbf{x}}_1).$$

Note that

$$\begin{aligned}F_{10}(\mathbf{h}_1) &= \sum_{\mathbf{x}_1\in X_1} f_{10}(\mathbf{x}_1)e_{\mathbf{A}_1}(\mathbf{h}_1, \mathbf{x}_1)\\ &= \sum_{\tilde{\mathbf{x}}_1\in\tilde{X}_1} f_{10}(\tilde{\mathbf{A}}_0\tilde{\mathbf{x}}_1)e_{\mathbf{A}_1}(\mathbf{h}_1, \tilde{\mathbf{A}}_0\tilde{\mathbf{x}}_1)\\ &\quad + e_{\mathbf{A}_1}(\mathbf{h}_1, \mathbf{e}_1)\sum_{\tilde{\mathbf{x}}_1\in\tilde{X}_1} f_{10}(\tilde{\mathbf{A}}_0\tilde{\mathbf{x}}_1 + \mathbf{e}_1)e_{\mathbf{A}_1}(\mathbf{h}_1, \tilde{\mathbf{A}}_0\tilde{\mathbf{x}}_1)\\ &= \sum_{\tilde{\mathbf{x}}_1\in\tilde{X}_1} f_{10,0}(\tilde{\mathbf{x}}_1)e_{\tilde{\mathbf{A}}_1}(\mathbf{h}_1, \tilde{\mathbf{x}}_1)\\ &\quad + e_{\mathbf{A}_1}(\mathbf{h}_1, \mathbf{e}_1)\sum_{\tilde{\mathbf{x}}_1\in\tilde{X}_1} f_{10,1}(\tilde{\mathbf{x}}_1)e_{\tilde{\mathbf{A}}_1}(\mathbf{h}_1, \tilde{\mathbf{x}}_1).\end{aligned}$$

Moreover, by (10),

$$F_{10}(\mathbf{h}_1) = F_{10,0}(\tilde{\mathbf{h}}_1) + e_{\mathbf{A}_1}(\mathbf{h}_1, \mathbf{e}_1)F_{10,1}(\tilde{\mathbf{h}}_1).$$

Since $f(x) = f(\mathbf{R}_\beta\mathbf{x})$ and

$$\begin{aligned}\mathbf{R}_\beta\{\mathbf{A}_0(\tilde{\mathbf{A}}_0\tilde{\mathbf{x}}_1 + \mathbf{e}_1) + \mathbf{e}_1\} &= \mathbf{A}_0\tilde{\mathbf{A}}_0\mathbf{R}_\beta\tilde{\mathbf{x}}_1 - 3\mathbf{e}_1\\ &= \mathbf{A}_0\tilde{\mathbf{A}}_0\mathbf{R}_\beta\tilde{\mathbf{x}}_1 - 4\mathbf{e}_1 + \mathbf{e}_1\\ &= \mathbf{A}_0\tilde{\mathbf{A}}_0(\mathbf{R}_\beta\tilde{\mathbf{x}}_1 - \mathbf{e}_1) + \mathbf{e}_1,\end{aligned}$$

it follows that

$$f_{10,1}(\tilde{\mathbf{x}}_1) = f_{10,0}(\mathbf{R}_\beta\tilde{\mathbf{x}}_1 - \mathbf{e}_1).$$

Hence,

$$\begin{aligned}F_{10,1}(\tilde{\mathbf{h}}_1) &= \sum_{\tilde{\mathbf{x}}_1\in\tilde{X}_1} f_{10,0}(\mathbf{R}_\beta\tilde{\mathbf{x}}_1 - \mathbf{e}_1)e_{\tilde{\mathbf{A}}_1}(\mathbf{R}_\beta^T\tilde{\mathbf{h}}_1, \mathbf{R}_\beta\tilde{\mathbf{x}}_1 - \mathbf{e}_1)\\ &\quad \times e_{\tilde{\mathbf{A}}_1}(\mathbf{R}_\beta^T\mathbf{h}_1, \mathbf{e}_1)\\ &= e_{\tilde{\mathbf{A}}_1}(\mathbf{R}_\beta^T\mathbf{h}_1, \mathbf{e}_1)F_{10,0}(\mathbf{R}_\beta^T\tilde{\mathbf{h}}_1).\end{aligned}$$

Moreover,

$$e_{\tilde{\mathbf{A}}_1}(\mathbf{R}_\beta^T\mathbf{h}_1, \mathbf{e}_1) = e_{\tilde{\mathbf{A}}_1}(\mathbf{h}_1, \mathbf{R}_\beta\mathbf{e}_1) = e_{\tilde{\mathbf{A}}_1}(\mathbf{h}_1, -\mathbf{e}_1)$$

and

$$\begin{aligned}e_{\mathbf{A}_1}(\mathbf{h}_1, \mathbf{e}_1)e_{\tilde{\mathbf{A}}_1}(\mathbf{h}_1, -\mathbf{e}_1) &= e_{\mathbf{A}_1}(\mathbf{h}_1, \mathbf{e}_1)e_{\mathbf{A}_1}(\mathbf{h}_1, -\tilde{\mathbf{A}}_0\mathbf{e}_1)\\ &= e_{\mathbf{A}_1}(\mathbf{h}_1, \mathbf{e}_1)e_{\mathbf{A}_1}(\mathbf{h}_1, -2\mathbf{e}_1)\\ &= e_{\mathbf{A}_1}(\mathbf{h}_1, -\mathbf{e}_1).\end{aligned}$$

[1] We excluded three from this example because for three the $p3$ symmetry reduction is a special case.

Consequently,

$$F_{10}(\mathbf{h}_1) = F_{10,0}(\tilde{\mathbf{h}}_1) + e_{\mathbf{A}_1}(\mathbf{h}_1, -\mathbf{e}_1)F_{10,0}(\mathbf{R}_\beta^T\tilde{\mathbf{h}}_1).$$

Therefore, taking into account equation (18), we see that it is sufficient to compute $F_{10,0}$ on $\frac{1}{8}$ of the data points and F_{00} on $\frac{1}{4}$ of the data points. To compute F_{00}, we decompose our grid again and again (reducing $p3$ symmetry first and the twofold symmetry induced by β) according to the factorization of N (Fig. 7).

Let us now go back to the point at which we obtained four subgrids as a result of the $p3$ symmetry reduction described by matrices $\mathbf{A}_0 = 2\mathbf{I}$ and $\mathbf{A}_1 = N\mathbf{I}$. Above we derived the formulae for the case of N even. If N is odd and is divisible by a prime number p such that $p > 2$, we would use the matrix

$$\tilde{\mathbf{A}}_0 = \begin{bmatrix} p & 0 \\ 0 & 1 \end{bmatrix}$$

to describe the decomposition of our computational grid into p subgrids. One can check that among these subgrids only the subgrid $\tilde{\mathbf{A}}_0\tilde{\mathbf{x}}_1 + [(p-1)/2]\mathbf{e}_1$ is invariant under the 180° rotation. Therefore, we have to compute the Fourier transform on $(p-1)/2$ grids with points in general position and on one grid with points in special positions. This SP grid should be decomposed again, this time along the y axis, to reduce the twofold symmetry. This algorithm is applied to the ITC groups 168–173 and, after reducing z-mirror symmetry, to the groups 175–182.

4.3. Diagonal mirror $-y, -x$ with no points on axes

The combination of the $p3$ symmetry and what we call here the 'diagonal mirror $-y, -x$' occurs for example in the crystallographic group $P3m1$. The algorithm for reducing $p3$ symmetry of a GP grid was described in detail in papers I and II. Now we will use the same algorithm, we only pick a different subgrid for further calculations. Specifically, as opposed to the previous case, where the Fourier transform was computed on a subgrid whose sum of coordinates was divisible by three, now we choose a subgrid whose sum of coordinates equals 2 modulo 3. Our motivation for a different choice is that we need a subgrid invariant with respect to the symmetry operator $-y, -x$. Unlike in the case of reducing $p3$ symmetry of a SP grid (described in §4.1) now we use a different grid coordinate system, given by

$$\mathbf{A} = 3N\begin{bmatrix} 1 & 0 \\ 0 & 1 \end{bmatrix} \quad \text{and} \quad \mathbf{b} = -\tfrac{1}{3}\begin{bmatrix} 2 \\ 1 \end{bmatrix}.$$

Moreover, the matrices $\mathbf{A}_0$ and $\mathbf{A}_1$ are also changed:

$$\mathbf{A}_0 = \begin{bmatrix} 3 & 0 \\ 0 & 3 \end{bmatrix} \quad \text{and} \quad \mathbf{A}_1 = \begin{bmatrix} N & 0 \\ 0 & N \end{bmatrix}.$$

As in §4.1, let us denote the 120 and 240° counterclockwise rotations around the origin of the crystallographic coordinate system by α and α^2, respectively. Let β denote the diagonal mirror operator $\bar{y}, \bar{x}$. Then the group $G = \{e, \alpha, \alpha^2, \beta, \beta\alpha, \beta\alpha^2\}$. The symmetry operators are given in the grid coordinates by

$$\mathbf{R}_\alpha = \begin{bmatrix} 0 & -1 \\ 1 & -1 \end{bmatrix} \quad \text{and} \quad \mathbf{t}_\alpha = \begin{bmatrix} -1 \\ 0 \end{bmatrix} \in \left[\begin{bmatrix} 2 \\ 0 \end{bmatrix}\right]_{\mathbf{A}_0} \tag{19}$$

$$\mathbf{R}_{\alpha^2} = \begin{bmatrix} -1 & 1 \\ -1 & 0 \end{bmatrix} \quad \text{and} \quad \mathbf{t}_{\alpha^2} = \begin{bmatrix} -1 \\ -1 \end{bmatrix} \in \left[\begin{bmatrix} 1 \\ 0 \end{bmatrix}\right]_{\mathbf{A}_0} \tag{20}$$

$$\mathbf{R}_\beta = \begin{bmatrix} 0 & -1 \\ -1 & 0 \end{bmatrix} \quad \text{and} \quad \mathbf{t}_\beta = \begin{bmatrix} -1 \\ -1 \end{bmatrix} \in \left[\begin{bmatrix} 1 \\ 0 \end{bmatrix}\right]_{\mathbf{A}_0}. \tag{21}$$

Let us also define

$$f_n m(\mathbf{x}_1) = f(\mathbf{A}_0\mathbf{x}_1 + n\mathbf{e}_1 + m\mathbf{e}_2),$$

where $\mathbf{x}_1 \in X_1$ and $n, m \in \{0, 1, 2\}$.

Let F_{nm} denote the Fourier transform of the function f_{nm},

$$F_{nm}(\mathbf{h}_1) = \sum_{\mathbf{x}_1 \in X_1} f_{nm}(\mathbf{x}_1)e_{\mathbf{A}_1}(\mathbf{h}_1, \mathbf{x}_1),$$

where $\mathbf{h}_1 \in \mathbb{Z}^2/\mathbf{A}_1^T\mathbb{Z}^2$. Then

$$F(\mathbf{h}) = \sum_{n=0}^{2}\sum_{m=0}^{2} e_{\mathbf{A}}(\mathbf{h}, n\mathbf{e}_1 + m\mathbf{e}_2)F_{nm}(\mathbf{h}_1).$$

With Γ_0 defined as usual, F_{02}, F_{20} and F_{11} are the Fourier transforms defined on subsets of the above-mentioned grid whose sum of coordinates equals 2 modulo 3. All other F_{nm}'s are related to them by symmetry operators. Let us now define

$$Y_2(\mathbf{h}_1) = e_{\mathbf{A}}(\mathbf{h}, 2\mathbf{e}_2)F_{02}(\mathbf{h}_1) + e_{\mathbf{A}}(\mathbf{h}, 2\mathbf{e}_1)F_{20}(\mathbf{h}_1) + e_{\mathbf{A}}(\mathbf{h}, \mathbf{e}_1 + \mathbf{e}_2)F_{11}(\mathbf{h}_1).$$

Note that here Y_2 denotes the Fourier transform of the subgrid $S_\alpha\Gamma_0$, rather than Γ_0, as in paper I. The reason we prefer $S_\alpha\Gamma_0$ over Γ_0 is that the former is invariant under the action of the symmetry operator β. We need to have a subgrid invariant under the action of β during this first decomposition because we will use it as a starting grid for the diagonal mirror decomposition in the second step. The subgrid Γ_0 is depicted in Fig. 8 by the blue triangles. The green triangles symbolize elements of $S_{\alpha^2}(\Gamma_0)$, while the yellow ones belong to $S_\alpha(\Gamma_0)$.

Now the Fourier transform F can be expressed in terms of Y_2:

$$F(\mathbf{h}) = Y_2(\mathbf{h}_1) + e_{\mathbf{A}}(\mathbf{h}, \mathbf{t}_\alpha)Y_2(\mathbf{R}_\alpha^T\mathbf{h}_1) + e_{\mathbf{A}}(\mathbf{h}, \mathbf{t}_{\alpha^2})Y_2(\mathbf{R}_{\alpha^2}^T\mathbf{h}_1).$$

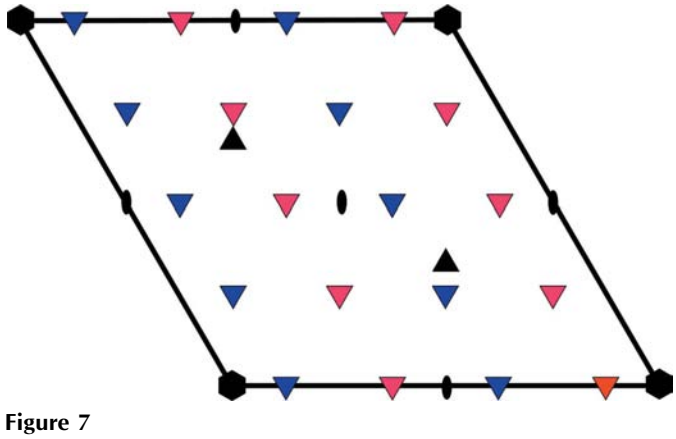

Figure 7
Subgrid decomposition of the $\mathbf{A}_0\mathbf{x}_1 + \mathbf{e}_1$ subgrid for the $p6$ symmetry in the case the number of points along x and y axes is divisible by 2.

We have to compute the Fourier transforms F_{02}, F_{20} and F_{11}. They are defined on different parts of $S_\alpha\Gamma_0$ and they all reveal the diagonal mirror symmetry due to the form the symmetry operator β has in the grid coordinates (21). In order to reduce this symmetry, if N is even, we apply formula (13), otherwise, we use a formula appropriate for the prime divisor p of N. A slight modification to the above formulae is needed since here we deal with diagonal mirror $\bar{y}, \bar{x}$ as opposed to y, x in §3. We will describe this algorithm using the example of even N. In this case, we introduce the new decomposition matrices $\tilde{\mathbf{A}}_0$ and $\tilde{\mathbf{A}}_1$:

$$\tilde{\mathbf{A}}_0 = \begin{bmatrix} 2 & 0 \\ 0 & 2 \end{bmatrix} \quad \text{and} \quad \tilde{\mathbf{A}}_1 = \begin{bmatrix} N/2 & 0 \\ 0 & N/2 \end{bmatrix}.$$

Then we perform another, finer, decomposition in the real space:

$$\mathbf{x}_1 = \tilde{\mathbf{A}}_0\tilde{\mathbf{x}}_1 + \tilde{\mathbf{x}}_0,$$

where $\tilde{\mathbf{x}}_0 \in \{\mathbf{0}, \mathbf{e}_1, \mathbf{e}_2, \mathbf{e}_1 + \mathbf{e}_2\}$ and $\tilde{\mathbf{x}}_1$ belongs to $\mathbb{Z}^2/\tilde{\mathbf{A}}_1\mathbb{Z}^2$. Let $f_{nm,jk}$ denote the function f_{nm} restricted to the (i, j)th subgrid (coming from the above decomposition) of the (n, m)th subgrid. Keeping in mind observation (10), let us now define

$$\begin{aligned}(F_{02,00})(\tilde{\mathbf{h}}_1) &= \sum_{\tilde{\mathbf{x}}_1\in\tilde{X}_1} (f_{02,00})(\tilde{\mathbf{x}}_1)e_{\tilde{\mathbf{A}}_1}(\tilde{\mathbf{h}}_1, \tilde{\mathbf{x}}_1) \\ &= \sum_{\tilde{\mathbf{x}}_1\in\tilde{X}_1} f_{02}(\tilde{\mathbf{A}}_0\tilde{\mathbf{x}}_1)e_{\tilde{\mathbf{A}}_1}(\mathbf{h}_1, \tilde{\mathbf{x}}_1) \\ &= \sum_{\tilde{\mathbf{x}}_1\in\tilde{X}_1} f(\mathbf{A}_0\tilde{\mathbf{A}}_0\tilde{\mathbf{x}}_1 + 2\mathbf{e}_2)e_{\tilde{\mathbf{A}}_1}(\mathbf{h}_1, \tilde{\mathbf{x}}_1),\end{aligned}$$

and analogously $F_{02,10}$, $F_{02,01}$ and $F_{02,11}$. Then

$$\begin{aligned}F_{02}(\mathbf{h}_1) = F_{02,00}(\tilde{\mathbf{h}}_1) &+ e_{\mathbf{A}_1}(\mathbf{h}_1, \mathbf{e}_1)F_{02,10}(\tilde{\mathbf{h}}_1) \\ &+ e_{\mathbf{A}_1}(\mathbf{h}_1, \mathbf{e}_2)F_{02,01}(\tilde{\mathbf{h}}_1) + e_{\mathbf{A}_1}(\mathbf{h}_1, \mathbf{e}_1 + \mathbf{e}_2)F_{02,11}(\tilde{\mathbf{h}}_1).\end{aligned}$$

Observe that, for $\mathcal{K} = 2\mathbf{e}_1$, $\mathcal{K} = \mathbf{e}_1 + \mathbf{e}_2$ or $\mathcal{K} = 2\mathbf{e}_2$, we have

$$S_\beta(\mathbf{A}_0\tilde{\mathbf{A}}_0\tilde{\mathbf{x}}_1 + \mathcal{K}) = \mathbf{A}_0(\tilde{\mathbf{A}}_0(S_\beta\tilde{\mathbf{x}}_1) + \mathbf{e}_1 + \mathbf{e}_2) + \mathcal{K}. \qquad (22)$$

Hence, since $f(S_\beta\mathbf{x}) = f(\mathbf{x})$ and $S_\beta^2 = \mathbf{I}$, we obtain

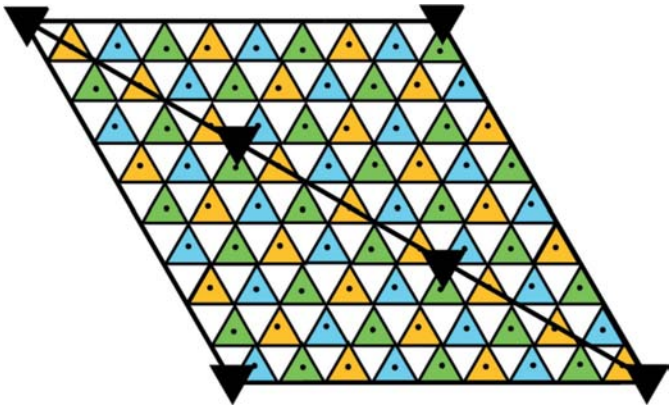

Figure 8
Subgrid decomposition for $p3$ group, for $N = 2$. The data point locations are symbolized by black dots. The subgrid $S_\alpha\Gamma_0$ consists of data points located in yellow triangles.

$$F_{02,00}(\tilde{\mathbf{h}}_1) = \sum_{\tilde{\mathbf{x}}_1\in\tilde{X}_1} f(S_\beta(\mathbf{A}_0\tilde{\mathbf{A}}_0\tilde{\mathbf{x}}_1 + 2\mathbf{e}_2))e_{\tilde{\mathbf{A}}_1}(\tilde{\mathbf{h}}_1, S_\beta^2\tilde{\mathbf{x}}_1).$$

By standard algebra, one can check that

$$e_{\tilde{\mathbf{A}}_1}(\tilde{\mathbf{h}}_1, S_\beta^2\tilde{\mathbf{x}}_1) = e_{\tilde{\mathbf{A}}_1}(\tilde{\mathbf{h}}_1, \mathbf{t}_\beta)e_{\tilde{\mathbf{A}}_1}(R_\beta^T\tilde{\mathbf{h}}_1, S_\beta\tilde{\mathbf{x}}_1).$$

From the above and (22), it follows that

$$\begin{aligned}&\sum_{\tilde{\mathbf{x}}_1\in\tilde{X}_1} f(S_\beta(\mathbf{A}_0\tilde{\mathbf{A}}_0\tilde{\mathbf{x}}_1 + 2\mathbf{e}_2))e_{\tilde{\mathbf{A}}_1}(\tilde{\mathbf{h}}_1, S_\beta^2\tilde{\mathbf{x}}_1) \\ &\quad = e_{\tilde{\mathbf{A}}_1}(\tilde{\mathbf{h}}_1, \mathbf{t}_\beta) \sum_{\tilde{\mathbf{x}}_1\in\tilde{X}_1} f(\mathbf{A}_0(\tilde{\mathbf{A}}_0S_\beta\tilde{\mathbf{x}}_1 + \mathbf{e}_1 + \mathbf{e}_2) + 2\mathbf{e}_2) \\ &\qquad \times e_{\tilde{\mathbf{A}}_1}(R_\beta^T\tilde{\mathbf{h}}_1, S_\beta\tilde{\mathbf{x}}_1) \\ &\quad = e_{\tilde{\mathbf{A}}_1}(\tilde{\mathbf{h}}_1, \mathbf{t}_\beta) \sum_{\tilde{\mathbf{x}}_1\in\tilde{X}_1} f_{02,11}(S_\beta\tilde{\mathbf{x}}_1)e_{\tilde{\mathbf{A}}_1}(R_\beta^T\tilde{\mathbf{h}}_1, S_\beta\tilde{\mathbf{x}}_1) \\ &\quad = e_{\tilde{\mathbf{A}}_1}(\tilde{\mathbf{h}}_1, \mathbf{t}_\beta)F_{02,11}(R_\beta^T\tilde{\mathbf{h}}_1).\end{aligned}$$

Therefore, the two transforms of the subgrids are symmetry related:

$$F_{02,00}(\tilde{\mathbf{h}}_1) = e_{\tilde{\mathbf{A}}_1}(\tilde{\mathbf{h}}_1, \mathbf{t}_\beta)F_{02,11}(R_\beta^T\tilde{\mathbf{h}}_1).$$

Analogously, we derive the remaining symmetry relations

$$F_{20,00}(\tilde{\mathbf{h}}_1) = e_{\tilde{\mathbf{A}}_1}(\tilde{\mathbf{h}}_1, \mathbf{t}_\beta)F_{20,11}(R_\beta^T\tilde{\mathbf{h}}_1)$$

and

$$F_{11,00}(\tilde{\mathbf{h}}_1) = e_{\tilde{\mathbf{A}}_1}(\tilde{\mathbf{h}}_1, \mathbf{t}_\beta)F_{11,11}(R_\beta^T\tilde{\mathbf{h}}_1).$$

Consequently, we can compute this partial Fourier transform using the formula

$$\begin{aligned}X(\mathbf{h}_1) = e_{\tilde{\mathbf{A}}_1}(\tilde{\mathbf{h}}_1, \mathbf{t}_\beta)X_{11}(\mathbf{R}_\beta^T\tilde{\mathbf{h}}_1) &+ e_{\mathbf{A}_1}(\mathbf{h}_1, \mathbf{e}_1 + \mathbf{e}_2)X_{11}(\tilde{\mathbf{h}}_1) \\ &+ e_{\mathbf{A}_1}(\mathbf{h}_1, \mathbf{e}_1)X_{10}(\tilde{\mathbf{h}}_1) + e_{\mathbf{A}_1}(\mathbf{h}_1, \mathbf{e}_2)X_{01}(\tilde{\mathbf{h}}_1),\end{aligned}$$

where $X = F_{02}$, F_{20} or F_{11}. The partial Fourier transforms X_{01} and X_{10} should be decomposed further.

This algorithm applies to the ITC groups 156, 158, 187, 188.

In this section, we have used the 'no special points' algorithm for the $p3$ symmetry from paper I, therefore, we had to assume that $\mathbf{A} = 3N\mathbf{I}$. To release this condition, we can always use the conceptually more complicated $p3$ algorithm with special points instead.

4.3.1. Reducing rhombohedral centering of the *p*3 symmetric SP grid. The algorithm for rhombohedral centering was described in paper III. It can be combined with the algorithm for $p3$ symmetry SP grid (ITC groups 148 and 155) in a manner similar to the $p3$ GP grid, which was described in detail in paper III.

5. Cubic groups

All cubic groups contain symmetry operators whose rotational parts are the same as those of the symmetry operators: $\bar{x}, \bar{y}, z$ and $\bar{x}, y, \bar{z}$. We will denote these operators by β and γ, respectively. The subgroup generated by these operators is $G = \{e, \beta, \gamma, \beta\gamma\}$. We begin by reducing the symmetry induced by these operators. Again, as in the other cases described in paper II and in this paper, the choice of an

algorithm depends most heavily on the rotational part of the symmetry operator. Therefore, even if the actual generators of a cubic group differ from β and γ by a translational part, it will incur only slight changes in our formulae, but the decomposition will remain the same.

Let us start again with a typical case, in which the grid size is divisible by 2. In the case of cubic groups, there is no dimension in which the symmetry operators act trivially, and the problem must be approached in three dimensions. We choose

$$\mathbf{A} = \begin{bmatrix} 2N & 0 & 0 \\ 0 & 2N & 0 \\ 0 & 0 & 2N \end{bmatrix} \quad \text{and} \quad \mathbf{b} = -\begin{bmatrix} 1/2 \\ 1/2 \\ 1/2 \end{bmatrix}$$

and

$$\mathbf{A}_0 = \begin{bmatrix} 2 & 0 & 0 \\ 0 & 2 & 0 \\ 0 & 0 & 2 \end{bmatrix} \quad \text{and} \quad \mathbf{A}_1 = \begin{bmatrix} N & 0 & 0 \\ 0 & N & 0 \\ 0 & 0 & N \end{bmatrix}.$$

It will soon be clear why we decompose the computational grid into eight subgrids, although the symmetry subgroup in question has only four elements. Let us also define

$$\Gamma = \mathbb{Z}^3/\mathbf{A}\mathbb{Z}^3 \quad \text{and} \quad X_1 = \mathbb{Z}^3/\mathbf{A}_1\mathbb{Z}^3.$$

The symmetry operators β and γ are described in grid coordinates by

$$\mathbf{R}_\beta = \begin{bmatrix} -1 & 0 & 0 \\ 0 & -1 & 0 \\ 0 & 0 & 1 \end{bmatrix} \quad \text{and} \quad \mathbf{t}_\beta = \begin{bmatrix} 1 \\ 1 \\ 0 \end{bmatrix}$$

$$\mathbf{R}_\gamma = \begin{bmatrix} -1 & 0 & 0 \\ 0 & 1 & 0 \\ 0 & 0 & -1 \end{bmatrix} \quad \text{and} \quad \mathbf{t}_\gamma = \begin{bmatrix} 1 \\ 0 \\ 1 \end{bmatrix}.$$

Moreover,

$$\mathbf{R}_{\beta\gamma} = \begin{bmatrix} 1 & 0 & 0 \\ 0 & -1 & 0 \\ 0 & 0 & -1 \end{bmatrix} \quad \text{and} \quad \mathbf{t}_{\beta\gamma} = \begin{bmatrix} 0 \\ 1 \\ 1 \end{bmatrix}.$$

Let us use the decomposition of $\mathbf{x}$, given by (3), to introduce eight new functions:

$$f_{nml}(\mathbf{x}_1) = f(\mathbf{A}_0\mathbf{x}_1 + n\mathbf{e}_1 + m\mathbf{e}_2 + l\mathbf{e}_3),$$

where $\mathbf{x}_1 \in X_1$ and $n, m, l \in \{0, 1\}$. Here, as in (24), $\Gamma_0 = \mathbf{A}_0 X_1$. The grid Γ_0 is colored red in Fig. 9.

Then, the Fourier transform F can be expressed as

$$\begin{aligned} F(\mathbf{h}) = {} & F_{000}(\mathbf{h}_1) + e_{\mathbf{A}}(\mathbf{h}, \mathbf{e}_1 + \mathbf{e}_2)F_{110}(\mathbf{h}_1) \\ & + e_{\mathbf{A}}(\mathbf{h}, \mathbf{e}_1 + \mathbf{e}_3)F_{101}(\mathbf{h}_1) + e_{\mathbf{A}}(\mathbf{h}, \mathbf{e}_2 + \mathbf{e}_3)F_{011}(\mathbf{h}_1) \\ & + e_{\mathbf{A}}(\mathbf{h}, \mathbf{e}_1)F_{100}(\mathbf{h}_1) + e_{\mathbf{A}}(\mathbf{h}, \mathbf{e}_2)F_{010}(\mathbf{h}_1) \\ & + e_{\mathbf{A}}(\mathbf{h}, \mathbf{e}_3)F_{001}(\mathbf{h}_1) + e_{\mathbf{A}}(\mathbf{h}, \mathbf{e}_1 + \mathbf{e}_2 + \mathbf{e}_3)F_{111}(\mathbf{h}_1). \end{aligned}$$

Moreover,

$$\begin{aligned} F_{000}(\mathbf{h}_1) &= e_{\mathbf{A}}(\mathbf{h}_1, \mathbf{t}_\beta)F_{110}(\mathbf{R}_\beta^T\mathbf{h}_1) \\ &= e_{\mathbf{A}}(\mathbf{h}_1, \mathbf{t}_\gamma)F_{101}(\mathbf{R}_\gamma^T\mathbf{h}_1) \\ &= e_{\mathbf{A}}(\mathbf{h}_1, \mathbf{t}_{\beta\gamma})F_{011}(\mathbf{R}_{\beta\gamma}^T\mathbf{h}_1). \end{aligned}$$

Analogously,

$$\begin{aligned} F_{111}(\mathbf{h}_1) &= e_{\mathbf{A}}(\mathbf{h}_1, \mathbf{t}_\beta)F_{001}(\mathbf{R}_\beta^T\mathbf{h}_1) \\ &= e_{\mathbf{A}}(\mathbf{h}_1, \mathbf{t}_\gamma)F_{010}(\mathbf{R}_\gamma^T\mathbf{h}_1) \\ &= e_{\mathbf{A}}(\mathbf{h}_1, \mathbf{t}_{\beta\gamma})F_{100}(\mathbf{R}_{\beta\gamma}^T\mathbf{h}_1). \end{aligned}$$

Hence,

$$\begin{aligned} F(\mathbf{h}) = {} & F_{000}(\mathbf{h}_1) + e_{\mathbf{A}}(\mathbf{h}_1, \mathbf{t}_\beta)e_{\mathbf{A}}(\mathbf{h}, \mathbf{e}_1 + \mathbf{e}_2)F_{000}(\mathbf{R}_\beta^T\mathbf{h}_1) \\ & + e_{\mathbf{A}}(\mathbf{h}_1, \mathbf{t}_\gamma)e_{\mathbf{A}}(\mathbf{h}, \mathbf{e}_1 + \mathbf{e}_3)F_{000}(\mathbf{R}_\gamma^T\mathbf{h}_1) \\ & + e_{\mathbf{A}}(\mathbf{h}_1, \mathbf{t}_{\beta\gamma})e_{\mathbf{A}}(\mathbf{h}, \mathbf{e}_2 + \mathbf{e}_3)F_{000}(\mathbf{R}_{\beta\gamma}^T\mathbf{h}_1) \\ & + e_{\mathbf{A}}(\mathbf{h}_1, \mathbf{t}_{\beta\gamma})e_{\mathbf{A}}(\mathbf{h}, \mathbf{e}_1)F_{111}(\mathbf{R}_{\beta\gamma}^T\mathbf{h}_1) \\ & + e_{\mathbf{A}}(\mathbf{h}_1, \mathbf{t}_\gamma)e_{\mathbf{A}}(\mathbf{h}, \mathbf{e}_2)F_{111}(\mathbf{R}_\gamma^T\mathbf{h}_1) \\ & + e_{\mathbf{A}}(\mathbf{h}_1, \mathbf{t}_\beta)e_{\mathbf{A}}(\mathbf{h}, \mathbf{e}_3)F_{111}(\mathbf{R}_\beta^T\mathbf{h}_1) \\ & + e_{\mathbf{A}}(\mathbf{h}, \mathbf{e}_1 + \mathbf{e}_2 + \mathbf{e}_3)F_{111}(\mathbf{h}_1). \end{aligned}$$

The symmetry will be reduced further if the space group contains the inversion operator $(\bar{x}, \bar{y}, \bar{z})$. The inversion symmetry operator ν is given in grid coordinates by

$$\mathbf{R}_\nu = \begin{bmatrix} -1 & 0 & 0 \\ 0 & -1 & 0 \\ 0 & 0 & -1 \end{bmatrix} \quad \text{and} \quad \mathbf{t}_\nu = \begin{bmatrix} 1 \\ 1 \\ 1 \end{bmatrix}.$$

Thus we arrive at the relationship between F_{000} and F_{111}:

$$F_{000}(\mathbf{h}_1) = e_{\mathbf{A}}(\mathbf{h}_1, \mathbf{t}_\nu)F_{111}(\mathbf{R}_\nu^T\mathbf{h}_1). \tag{23}$$

Alternatively, the Hermitian symmetry can be used in this step if the input data are all real numbers (§7). We will proceed now to reducing the $P3$ symmetry. All cubic groups contain symmetry operators y, z, x and z, x, y (*i.e.* 120 and 240° counterclockwise rotations around the main diagonal), described in the grid coordinates by

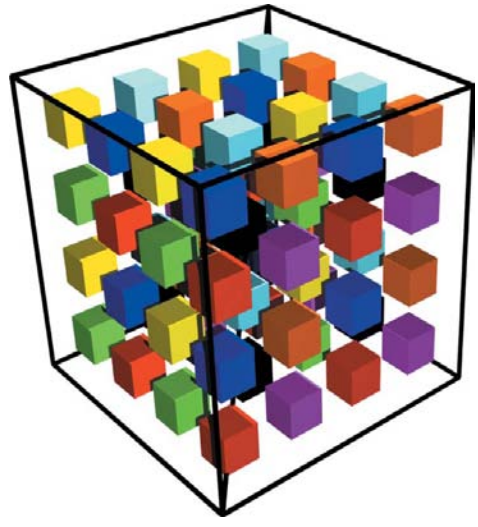

Figure 9
Subgrid decomposition for a cubic group for $N = 2$. The data points are located in the centers of cubes. The asymmetric unit Γ_0 is represented by the eight red cubes.

$$\mathbf{R}_\alpha = \begin{bmatrix} 0 & 1 & 0 \\ 0 & 0 & 1 \\ 1 & 0 & 0 \end{bmatrix} \quad \text{and} \quad \mathbf{R}_{\alpha^2} = \begin{bmatrix} 0 & 0 & 1 \\ 1 & 0 & 0 \\ 0 & 1 & 0 \end{bmatrix}$$

and $\mathbf{t}_\alpha = \mathbf{t}_{\alpha^2} = \mathbf{0}$. To reduce the symmetry induced by these operators, we will use the function f_{000} from the previous stage (if there is no inversion in the space group and Hermitian symmetry is not present, both f_{000} and f_{111} will be needed). So far, we have reduced symmetry eight times and we have only to compute the Fourier transform F_{000}. Assuming that N is even, we can choose $\tilde{\mathbf{A}}_0 = 2\mathbf{I}$ and $\tilde{\mathbf{A}}_1 = (N/2)\mathbf{I}$. Let us decompose $\mathbf{x}_1$, according to rule (3), to introduce eight new functions:

$$f_{000,nml}(\tilde{\mathbf{x}}_1) = f_{000}(\tilde{\mathbf{A}}_0\tilde{\mathbf{x}}_1 + n\mathbf{e}_1 + m\mathbf{e}_2 + l\mathbf{e}_3),$$

where $\tilde{\mathbf{x}}_1 \in \mathbb{Z}^3/\tilde{\mathbf{A}}_1\mathbb{Z}^3$ and $n, m, l \in \{0, 1\}$. This decomposition is depicted in Fig. 10.

To avoid excessive subscripts, from now on we omit the first subscript 000, that is F stands for F_{000}. Then, the Fourier transform F can be expressed as

$$\begin{aligned} F(\mathbf{h}_1) = {} & F_{000}(\tilde{\mathbf{h}}_1) + e_{\mathbf{A}_1}(\mathbf{h}_1, \mathbf{e}_1 + \mathbf{e}_2)F_{110}(\tilde{\mathbf{h}}_1) \\ & + e_{\mathbf{A}_1}(\mathbf{h}_1, \mathbf{e}_1 + \mathbf{e}_3)F_{101}(\tilde{\mathbf{h}}_1) + e_{\mathbf{A}_1}(\mathbf{h}_1, \mathbf{e}_2 + \mathbf{e}_3)F_{011}(\tilde{\mathbf{h}}_1) \\ & + e_{\mathbf{A}_1}(\mathbf{h}_1, \mathbf{e}_1)F_{100}(\tilde{\mathbf{h}}_1) + e_{\mathbf{A}_1}(\mathbf{h}_1, \mathbf{e}_2)F_{010}(\tilde{\mathbf{h}}_1) \\ & + e_{\mathbf{A}_1}(\mathbf{h}_1, \mathbf{e}_3)F_{001}(\tilde{\mathbf{h}}_1) + e_{\mathbf{A}_1}(\mathbf{h}_1, \mathbf{e}_1 + \mathbf{e}_2 + \mathbf{e}_3)F_{111}(\tilde{\mathbf{h}}_1). \end{aligned}$$

Moreover,

$$F_{100}(\tilde{\mathbf{h}}_1) = F_{001}(\mathbf{R}_\alpha^T\tilde{\mathbf{h}}_1) = F_{010}(\mathbf{R}_{\alpha^2}^T\tilde{\mathbf{h}}_1).$$

Analogously,

$$F_{110}(\tilde{\mathbf{h}}_1) = F_{101}(\mathbf{R}_\alpha^T\tilde{\mathbf{h}}_1) = F_{011}(\mathbf{R}_{\alpha^2}^T\tilde{\mathbf{h}}_1).$$

Hence, the final formula is

$$\begin{aligned} F(\mathbf{h}_1) = {} & F_{000}(\tilde{\mathbf{h}}_1) + e_{\mathbf{A}_1}(\mathbf{h}_1, \mathbf{e}_1 + \mathbf{e}_2)F_{110}(\tilde{\mathbf{h}}_1) \\ & + e_{\mathbf{A}_1}(\mathbf{h}_1, \mathbf{e}_1 + \mathbf{e}_3)F_{110}(\mathbf{R}_{\alpha^2}^T\tilde{\mathbf{h}}_1) \\ & + e_{\mathbf{A}_1}(\mathbf{h}_1, \mathbf{e}_2 + \mathbf{e}_3)F_{110}(\mathbf{R}_\alpha^T\tilde{\mathbf{h}}_1) \\ & + e_{\mathbf{A}_1}(\mathbf{h}_1, \mathbf{e}_1)F_{001}(\mathbf{R}_\alpha^T\tilde{\mathbf{h}}_1) + e_{\mathbf{A}_1}(\mathbf{h}_1, \mathbf{e}_2)F_{001}(\mathbf{R}_{\alpha^2}^T\tilde{\mathbf{h}}_1) \\ & + e_{\mathbf{A}_1}(\mathbf{h}_1, \mathbf{e}_3)F_{001}(\tilde{\mathbf{h}}_1) + e_{\mathbf{A}_1}(\mathbf{h}_1, \mathbf{e}_1 + \mathbf{e}_2 + \mathbf{e}_3)F_{111}(\tilde{\mathbf{h}}_1). \end{aligned}$$

This formula resembles the one for $F(\mathbf{h})$ but note that now the relationships between Fourier transforms of the subgrids are different. Namely, this time one has to compute the Fourier transforms F_{100} and F_{110} and decompose further F_{000} and F_{111}. If N is a power of 2, then this next decomposition will be exactly the same as above. If N has a different prime-factor decomposition, then it is sufficient to slightly alter this scheme, as with other described algorithms. For example, if prime factor is 3, out of 27 Fourier transforms we compute only 8: F_{100}, F_{110}, F_{200}, F_{220}, F_{122}, F_{112}, F_{120} and F_{210}, and we decompose further F_{000}, F_{111} and F_{222}.

The formulae here were derived for ITC group 200, that is $Pm\bar{3}$. The ITC space groups 197, 201, 205, 207, 208, 212, 213 differ from 200 only in that their generating symmetry operators have different translational parts, therefore there has to be a change in the coefficients in the above formulae reflecting it. For the space groups where there is no inversion, *e.g.* ITC group 195 ($P23$), we will use Hermitian symmetry to derive relationship between F_{000} and F_{111} (§7). If the Hermitian symmetry is not present either, we have to compute both

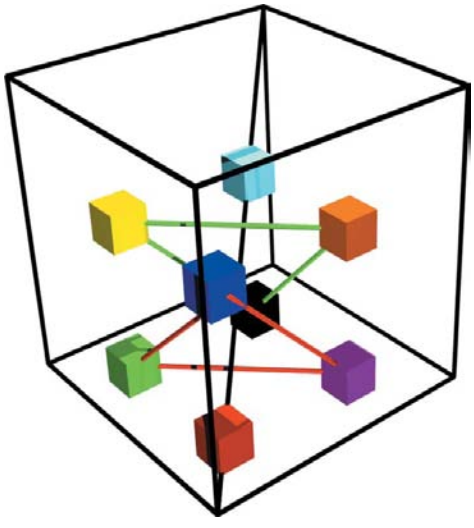

Figure 10
Subgrid decomposition for a cubic group for $N = 2$. The data points are located in the centers of colored cubes.

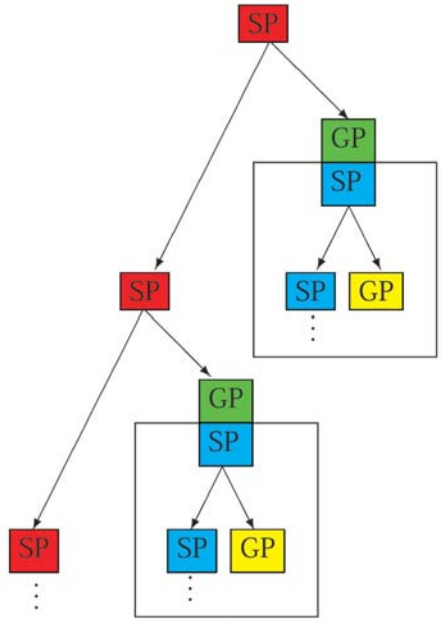

Figure 11
Decomposition in the case of two consecutive recursive symmetry decompositions with respect to different symmetry subgroups. In such a case, a GP grid with respect to one symmetry can be a SP grid with respect to the other. As such, it will be decomposed again but according to different rules. SP and GP grids with respect to the symmetry applied first are colored red and green, respectively. SP and GP grids with respect to the other symmetry are colored blue and yellow. For simplicity, grids that are GP grids with respect to both symmetries have been omitted.

F_{000} and F_{111} from the first stage. Reducing the internal symmetry of F_{111} is exactly the same as that of F_{000}.

For groups 215–230, we have to combine this algorithm with diagonal mirror-symmetry reduction. To this end, observe that both F_{001} and F_{110} (from the trigonal symmetry reduction stage) preserve diagonal mirror symmetry, so they can be decomposed further as in the diagonal mirror algorithm (§3). Combining several recursive symmetry decompositions will be discussed in the next section.

For some space groups, we have also to reduce centering. The discussed algorithm can be combined with body centering or with face centering according to the general rules, as described in paper III.

6. Combining several recursive symmetry-reduction algorithms

As we saw at the end of the previous section, for some groups we have to combine several recursive symmetry decompositions. Such a combination is rather straightforward (Fig. 11).

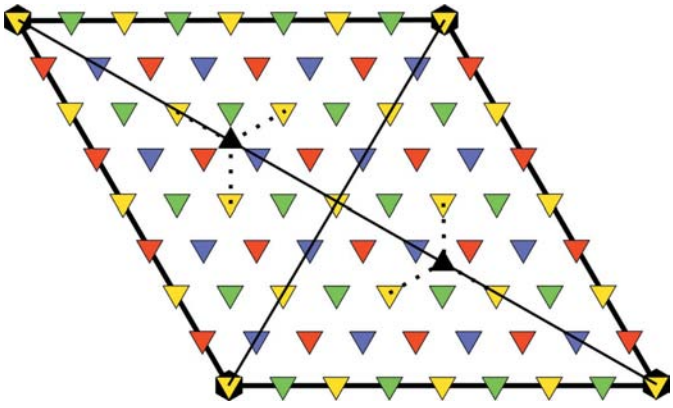

Figure 12
Decomposition of the SP grid with respect to $p3$ symmetry. The number of grid points is even, but not divisible by three. The blue subgrid is a GP subgrid with respect to $p3$ symmetry but is a SP subgrid with respect to both the y, x and $\bar{y}, \bar{x}$ symmetry operators.

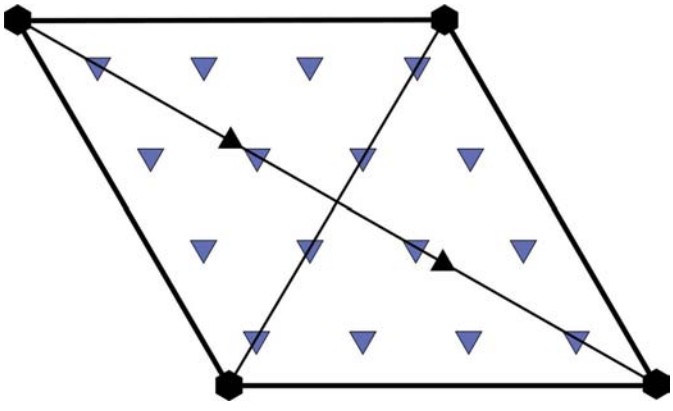

Figure 13
A $p3$ GP subgrid invariant with respect to both intersecting diagonal mirrors. This subgrid is decomposed further.

6.1. Intersecting diagonal mirrors combined with $p3$ symmetry

The most complicated combination of symmetries arises when intersecting diagonal mirrors are combined with the $p3$ symmetry. Such a combination of symmetries can be found in ITC groups 183–186 and 191–194. Reducing this symmetry requires three recursive decompositions with respect to different sets of operators.

We first perform a decomposition with respect to the $p3$ symmetry and as a result we obtain four subgrids, three of which are GP subgrids with respect to this symmetry, and the fourth one is a SP subgrid. Since the three GP subgrids are symmetry related, it is sufficient to consider one of them. We choose the one that is invariant with respect to both y, x and $\bar{y}, \bar{x}$ diagonal mirror-symmetry operators (blue subgrid in Fig. 12).

We will not discuss the SP grid with respect to the $p3$ symmetry, as it can be decomposed further according to the $p3$ recursive symmetry algorithm described earlier. Let us instead focus on the GP subgrid that is invariant with respect to both intersecting diagonal mirrors (see Fig. 13).

As before, we will perform a step-by-step reduction of the symmetry of this subgrid. Let us start with reducing the symmetry related to the diagonal mirror y, x. To this end, let us decompose the GP grid obtained from the previous step, which is a SP grid with respect to the diagonal mirror y, x symmetry. For simplicity, we assume that the number of points in this GP grid is even. We apply the usual diagonal mirror decomposition (§3). Since the trigonal symmetry has already been reduced, we draw the asymmetric unit as a square, which we find more convenient for the purpose of illustrating the diagonal mirror symmetry (Fig. 14). The red subgrid $(0, 0)$ in Fig. 14 is a symmetric image of the green subgrid $(1, 1)$ in the diagonal mirror $\bar{y}, \bar{x}$. On the other hand, the yellow subgrid $(0, 1)$ is a symmetric image of the blue subgrid $(1, 0)$ in the diagonal mirror y, x. Therefore, it is sufficient to consider further the red grid and the blue grid. The blue subgrid $(1, 0)$

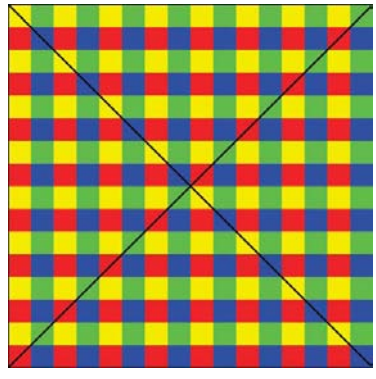

Figure 14
Decomposition of the blue subgrids from Fig. 13 with respect to the diagonal mirror y, x symmetry. The blue and yellow subgrids are GP, red and green are SP with respect to the diagonal mirror y, x. However, yellow and blue grids are SP, and the other two are GP with respect to the other diagonal mirror symmetry. For clarity, the decomposition is presented on a rectangular grid and there are more points than in Fig. 13.

no longer reveals the y, x symmetry, but it still possesses the $\bar{y}, \bar{x}$ symmetry. Therefore, it can be decomposed again, as in Fig. 15. At this point, the only remaining symmetry is induced by the single diagonal mirror, and it is sufficient to apply the algorithm described in §3.

Let us now go back to the red grid (0, 0) from Fig. 13. This grid reveals the diagonal mirror y, x symmetry and will be decomposed in a manner similar to the previous one (Fig. 16). Thus the symmetry will eventually be reduced completely.

6.2. Similar algorithms

The algorithm for reducing the $p3$ symmetry on a SP grid can be combined with reducing the z-mirror symmetry (paper II), or with rhombohedral centering (paper III).

7. Hermitian symmetry

So far, we have discussed the complex-to-complex crystallographic Fourier transform. To apply our algorithm to actual crystallographic data, where electron density is represented by real numbers, one needs to combine the crystallographic symmetry reduction with Hermitian symmetry, which imposes the following relation in the reciprocal space:

$$\overline{F(\mathbf{h})} = F(-\mathbf{h}).$$

Since the Hermitian-symmetry reduction is very similar to any other symmetry-reduction step, it can be combined with the others using the general rules described earlier in this paper. Of course, since the crystallographic symmetry reduction algorithm deals with complex numbers, the Hermitian symmetry reduction should be applied first. In most cases, a direction can be selected such that two real numbers neighboring along this direction are 'packed' together into one complex number, and the real and imaginary subgrids have the same symmetry properties. Only in some cubic groups will the first step be different (Table 2, Appendix B). In these cases, the reduction of the fourfold orthorhombic symmetry can be combined with the reduction of the Hermitian symmetry into one simple step (denoted by H8 in Appendix B). The Hermitian symmetry simplifies the problem in a very similar way to the inversion. For example, for the case discussed in §5, the Hermitian symmetry introduces the relationship

$$\overline{F_{000}(\mathbf{h}_1)} = F_{111}(-\mathbf{h}_1),$$

which allows for an efficient symmetry reduction (23). The problem is thus reduced to solving rhombohedral symmetry. In some space groups, the residual rhombohedral symmetry will include additional centering. In such a case, one can start with complex-to-complex symmetry reduction, as described in Appendix B, and combine it with the Hermitian symmetry reduction using general rules. Alternatively, one can combine reducing Hermitian symmetry with reduction of orthorhombic symmetry or centering, as sketched above.

Since our choice of the coordinate system in the real space, and the symmetry reduction methods described above, ensure that in real space there are no SP grids except for one-point grids, the Hermitian symmetry reduction in the real space is straightforward. In the reciprocal space, however, we have to deal with issues that are not encountered with a classical choice of coordinate system.

The FFT asymmetric units in the reciprocal space that are compatible with our symmetry reduction methods have been described in detail in paper IV. We have also presented there a general algorithm that resulted in an optimal FFT asymmetric unit in the reciprocal space for complex-to-complex data and any grid sizes for all crystallographic groups, for which one-step symmetry reduction is applicable (paper II). We have shown that the shapes of FFT asymmetric units in the reciprocal space can be generated by careful management of special points (systematic absences).

The Hermitian symmetry introduces one new class of special points, namely 'fixed phase' points $\mathbf{h}$, for which there exists a $g \in G$ such that

$$[-\mathbf{R}_g^T\mathbf{h}]_{\mathbf{A}^T} = \mathbf{h},$$

where $[-\mathbf{R}_g^T\mathbf{h}]_{\mathbf{A}^T}$ denotes the equivalence class of a vector $-\mathbf{R}_g^T\mathbf{h}$ with respect to matrix $\mathbf{A}^T$ (paper IV), that is

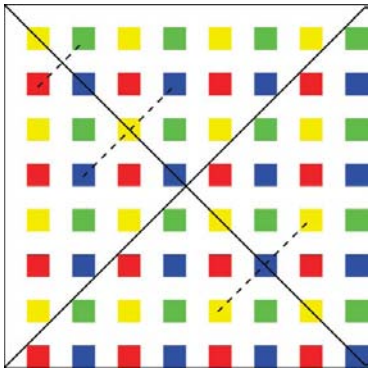

Figure 15
Decomposition of the blue subgrids from Fig. 14. Blue and yellow subgrids are invariant for diagonal mirror $\bar{y}, \bar{x}$ symmetry, while the green and red subgrids are symmetry related for this symmetry.

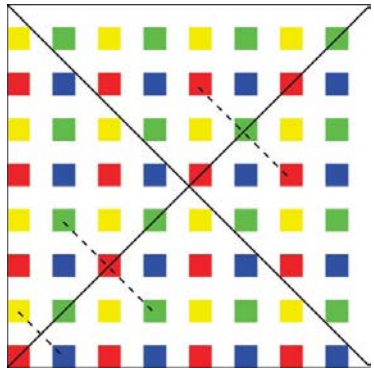

Figure 16
Decomposition of the red subgrid from Fig. 14. Red and green subgrids are symmetry invariant, while yellow and blue subgrids are symmetry related for the diagonal mirror y, x.

$$[\mathbf{h}]_{\mathbf{A}^T} := \{\mathbf{k} \in \mathbb{Z}^3 : \mathbf{k} - \mathbf{h} \in \mathbf{A}^T\mathbb{Z}^3\}.$$

Then, remembering that, for all elements g of the crystallographic group G, $S_g^* F(\mathbf{h}) = F(\mathbf{h})$ and from the general formula

$$S_g^* F(\mathbf{h}) = \exp(-2\pi i \mathbf{h} \cdot \mathbf{A}^{-1}\mathbf{t}_g) F(\mathbf{R}_g^T \mathbf{h})$$

one can derive that, regardless of the real-space data, the phase of $F(\mathbf{h})$ is fixed:

$$\arg(F(\mathbf{h})) = -\pi \mathbf{h} \cdot \mathbf{A}^{-1}\mathbf{t}_g.$$

The simplest case of fixed phase points are those with only real or only imaginary parts. The number of fixed-phase points is always even and they can be managed by packing in pairs, choosing partners that are multiplied by similar coefficients (twiddle factors) during Fourier transform (*e.g.* ones that differ by π or $\pi/2$). This procedure naturally extends our recipe for the FFT asymmetric unit (ASU) presented in paper IV (Kudlicki *et al.*, 2004), with the size of the FFT ASU additionally reduced by half. Such an approach ensures a completely optimal in-place crystallographic FFT.

8. Discussion

This paper completes the presentation of the theoretical foundations of algorithms for fully efficient crystallographic FFT. Now all the crystallographic symmetries have been covered, as summarized in the tables in the present paper and in papers II and III. The choice of appropriate FFT ASU in reciprocal space is described in paper IV. In this paper, we presented the recursive symmetry decomposition, which we use to reduce the crystallographic symmetry when grid points in special positions are present. The recursive symmetry decomposition is more general than the decompositions discussed previously. Since we no longer require that the grid contains no special points, we can apply this algorithm to any crystallographic group, not only to those included in Appendix *B*. Also, one can construct a recursive algorithm for any number of points along unit-cell edges, however, the calculations are both faster and simpler when these numbers are products of small primes. We have drawn attention to these two observations while discussing the *p*3 symmetry in §4.1.

The one-step algorithms described previously are used as building blocks for the recursive ones, which could not exist without them. This recursive decomposition should be thought of as a method of reducing the general case to the 'no special points case' applied several times. Moreover, the one-step algorithms can work with simpler data structures and loop organization, so they should be chosen whenever both alternatives are possible.

The recursive algorithms are more complicated than algorithms presented before but they still can be built from simple pieces. Unlike in one-step symmetry reduction, details of these algorithms strongly depend on the prime-factor decomposition of the number of grid points in the unit cell.

Our symmetric FFT is a generalization of the Cooley–Tukey algorithm, and most implementation issues are characteristic of non-crystallographic Cooley–Tukey routines. The recursive algorithms presented here can be implemented as a series of three-dimensional *P*1 FFT's, supplied with symmetry-reduction steps. Since the computational complexity of the symmetry reduction is $\mathcal{O}(N)$, the majority of calculations performed are in the *P*1 FFT step. Moreover, both in the symmetry reduction and in the *P*1 calculation, the memory access patterns are regular, which makes them compatible with efficient stride-based cache prefetching. The crystallographic FFT will thus benefit from application of generic highly optimized fast Fourier transform implementations.

APPENDIX *A*
The symmetry-reduction formula

The formula that allows the multi-dimensional Cooley–Tukey factorization to be combined with crystallographic symmetry was derived by Bricogne (1993) and, under weaker assumptions, in paper II. Such algorithms have to be group specific. Let $\mathbf{A}$ be the matrix describing the periodic computational grid. Then $|\det \mathbf{A}|$ is the number of points in the unit cell. Suppose that for the quotient crystallographic group G there exist matrices $\mathbf{A}_0$ and $\mathbf{A}_1$ satisfying (2). Suppose also that these matrices are such that the number of elements of G, denoted by $|G|$, equals $|\det \mathbf{A}_1|$:

$$|G| = |\det \mathbf{A}_1|.$$

Let Γ_0 denote

$$\Gamma_0 = \mathbf{A}_0 X_1. \tag{24}$$

Let f be any function on Γ that respects the crystallographic symmetry, that is such that

$$f(\mathbf{x}) = f(S_g \mathbf{x}) \tag{25}$$

for any $x \in \Gamma$ and $g \in G$.

We will require that the following assumptions are satisfied.

1. The grid Γ can be expressed as a sum of $|G|$ mutually disjoint sets $S_{g_i}\Gamma_0$, where $g_i \in G$, that is

$$S_{g_1}\Gamma_0 \cap S_{g_2}\Gamma_0 = \emptyset \text{ for } g_1 \neq g_2$$

and

$$\Gamma = \bigcup_{g \in G} S_g \Gamma_0. \tag{26}$$

Then,

$$|\Gamma| = |G||\Gamma_0|.$$

2. For every $g \in G$ we have:

$$S_g(\Gamma_0) = [\mathbf{t}_g]_{\Gamma_0} = \{\mathbf{x} \in \Gamma : \mathbf{x} = \gamma + \mathbf{t}_g \quad \text{and} \quad \gamma \in \Gamma_0\}.$$

3. Matrix $\mathbf{A}$ commutes with $\mathbf{R}_g$ for every $g \in G$:

$$\mathbf{A}\mathbf{R}_g = \mathbf{R}_g\mathbf{A}.$$

Table 1
Algorithms for recursive crystallographic symmetry reduction.

Columns 1 and 2: crystallographic group number and symbol; column 3: number of elements; columns 4, 5 6, 7: algorithm types (for one-step symmetry reduction algorithms and reducing centering see papers II and III, respectively).

No.	Name	$\|G\|$	Algorithm: steps			
99	$P4mm$	8	yx	2x2y		
100	$P4bm$	8	yx	2x2y		
101	$P4_2cm$	8	yx	2x2y		
102	$P4_2nm$	8	yx	2x2y		
103	$P4cc$	8	yx	2x2y		
104	$P4nc$	8	yx	2x2y		
105	$P4_2mc$	8	yx	2x2y		
106	$P4_2bc$	8	yx	2x2y		
107	$I4mm$	16	yx	2x2y	ICent	
108	$I4cm$	16	yx	2x2y	ICent	
109	$I4_1md$	16	yx	2x2y	ICent	
110	$I4_1cd$	16	yx	2x2y	ICent	
111	$P\bar{4}2m$	8	yx	2x2y		
112	$P\bar{4}2c$	8	yx	2x2y		
113	$P\bar{4}2_1m$	8	yx	2x2y		
114	$P\bar{4}2_1c$	8	yx	2x2y		
121	$I\bar{4}2m$	16	yx	2x2y	ICent	
122	$I\bar{4}2d$	16	yx	2x2y	ICent	
123	$P4/mmm$	16	yx	2x2y2z		
124	$P4/mcc$	16	yx	2x2y2z		
125	$P4/nbm$	16	yx	2x2y2z		
126	$P4/nnc$	16	yx	2x2y2z		
127	$P4/mbm$	16	yx	2x2y2z		
128	$P4/mnc$	16	yx	2x2y2z		
129	$P4/nmm$	16	yx	2x2y2z		
130	$P4/ncc$	16	yx	2x2y2z		
131	$P4_2/mmc$	16	yx	2x2y2z		
132	$P4_2/mcm$	16	yx	2x2y2z		
133	$P4_2/nbc$	16	yx	2x2y2z		
134	$P4_2/nnm$	16	yx	2x2y2z		
135	$P4_2/mbc$	16	yx	2x2y2z		
136	$P4_2/mnm$	16	yx	2x2y2z		
137	$P4_2/nmc$	16	yx	2x2y2z		
138	$P4_2/ncm$	16	yx	2x2y2z		
139	$I4/mmm$	32	yx	2x2y2z	ICent	
140	$I4/mcm$	32	yx	2x2y2z	ICent	
141	$I4_1/amd$	32	yx	2x2y2z	ICent	
142	$I4_1/acd$	32	yx	2x2y2z	ICent	
147	$P\bar{3}$	6	P3a	2z		
148	$R\bar{3}$	18	P3a	2z	RCent	
150	$P321$	6	P3a	2z		
152	$P3_121$	6	P3a	2z		
154	$P3_221$	6	P3a	2z		
155	$R32$	18	P3a	2z	RCent	
156	$P3m1$	6	3(x+y)	−y−x		
157	$P31m$	6	P3a	yx		
158	$P3c1$	6	3(x+y)	−y−x		
159	$P31c$	6	P3a	yx		
160	$R3m$	18	3(x+y)	−y−x	RCent	
161	$R3c$	18	3(x+y)	−y−x	RCent	
162	$P\bar{3}1m$	12	P3a	yx	2z	
163	$P\bar{3}1c$	12	P3a	yx	2z	
164	$P\bar{3}m1$	12	P3a	yx	2z	
165	$P\bar{3}c1$	12	P3a	yx	2z	
166	$R\bar{3}m$	36	P3a	−y−x	2z	RCent
167	$R\bar{3}c$	36	P3a	−y−x	2z	RCent
168	$P6$	6	P6			
169	$P6_1$	6	P6			
170	$P6_5$	6	P6			
171	$P6_2$	6	P6			
172	$P6_4$	6	P6			
173	$P6_3$	6	P6			
175	$P6/m$	12	P6	2z		
176	$P6_3/m$	12	P6	2z		
177	$P622$	12	P6	2z		
178	$P6_122$	12	P6	2z		
179	$P6_522$	12	P6	2z		
180	$P6_222$	12	P6	2z		
181	$P6_422$	12	P6	2z		
182	$P6_322$	12	P6	2z		
183	$P6mm$	12	P3a	yx	−y−x	
184	$P6cc$	12	P3a	yx	−y−x	
185	$P6_3cm$	12	P3a	yx	−y−x	
186	$P6_3mc$	12	P3a	yx	−y−x	
187	$P\bar{6}m2$	12	3(x+y)	−y−x	2z	
188	$P\bar{6}c2$	12	3(x+y)	−y−x	2z	
189	$P\bar{6}2m$	12	P3a	yx	2z	
190	$P\bar{6}2c$	12	P3a	yx	2z	
191	$P6/mmm$	24	P3a	yx	−y−x	2z
192	$P6/mcc$	24	P3a	yx	−y−x	2z
193	$P6_3/mcm$	24	P3a	yx	−y−x	2z
194	$P6_3/mmc$	24	P3a	yx	−y−x	2z
195	$P23$	12	A8(2)	P3c		
196	$F23$	48	A8(2)	P3c	FCent	
197	$I23$	24	A8(1)	P3c		
198	$P2_13$	12	A8(2)	P3c		
199	$I2_13$	24	A8(2)	P3c	ICent	
200	$Pm\bar{3}$	24	A8(1)	P3c		
201	$Pn\bar{3}$	24	A8(1)	P3c		
202	$Fm\bar{3}$	96	A8(1)	P3c	FCent	
203	$Fd\bar{3}$	96	A8(1)	P3c	FCent	
204	$Im\bar{3}$	48	A8(1)	P3c	ICent	
205	$Pa\bar{3}$	24	A8(1)	P3c		
206	$Ia\bar{3}$	48	A8(1)	P3c	ICent	
207	$P432$	24	A8(1)	P3c		
208	$P4_232$	24	A8(1)	P3c		
209	$F432$	96	A8(1)	P3c	FCent	
210	$F4_132$	96	A8(1)	P3c	FCent	
211	$I432$	48	A8(1)	P3c	ICent	
212	$P4_332$	24	A8(1)	P3c		
213	$P4_132$	24	A8(1)	P3c		
214	$I4_132$	48	A8(1)	P3c	ICent	
215	$P\bar{4}3m$	24	A8(2)	P3c	yx	
216	$F\bar{4}3m$	96	A8(2)	P3c	yx	FCent
217	$I\bar{4}3m$	48	A8(2)	P3c	yx	ICent
218	$P\bar{4}3n$	24	A8(2)	P3c	yx	
219	$F\bar{4}3c$	96	A8(2)	P3c	yx	FCent
220	$I\bar{4}3d$	48	A8(2)	P3c	yx	ICent
221	$Pm\bar{3}m$	48	A8(1)	P3c	yx	
222	$Pn\bar{3}n$	48	A8(1)	P3c	yx	
223	$Pm\bar{3}n$	48	A8(1)	P3c	yx	
224	$Pn\bar{3}m$	48	A8(1)	P3c	yx	
225	$Fm\bar{3}m$	192	A8(1)	P3c	yx	FCent
226	$Fm\bar{3}c$	192	A8(1)	P3c	yx	FCent
227	$Fd\bar{3}m$	192	A8(1)	P3c	yx	FCent
228	$Fd\bar{3}c$	192	A8(1)	P3c	yx	FCent
229	$Im\bar{3}m$	96	A8(1)	P3c	yx	ICent
230	$Ia\bar{3}d$	96	A8(1)	P3c	yx	ICent

Symbol explanation. 2x: regular subgrid consisting of every second point along the x axis. 2x2y: regular subgrid consisting of every second point along x and y axes. 2x2y2z: regular subgrid consisting of every second point along x, y and z axes (paper II). yx, −y−x: diagonal mirror. 3(x+y): subgrid of $x + y$ divisible by 3 (reducing $p3$ symmetry of GP grid, §4.3). ICent: body centering (paper III). FCent: all-face centering (paper III). P3a: recursive trigonal with points on axes (reducing $p3$ symmetry of SP grid), §4.1. P3c: same, axis along cube diagonal, §5. P6: recursive algorithm for hexagonal set-up (with data on axes), §4.2. RCent: rhombohedral centering (paper III). A8(1), A8(2): same as 2x2y2z, with further decomposition of 1 (with inversion) or 2 (if there is no inversion) out of 8 subgrids, §5.

Here, Γ_0 plays the role of the asymmetric unit. Let us introduce the symbol $Y(\mathbf{h}_1)$ for the Fourier transform of the data in the asymmetric unit Γ_0,

$$Y(\mathbf{h}_1) = \sum_{\gamma \in \Gamma_0} f(\gamma) e_{\mathbf{A}}(\mathbf{h}_1, \gamma).$$

Table 2
Algorithms for recursive crystallographic symmetry reduction specific to Hermitian symmetry.

Columns as in Table 1.

No.	Name	$\|G\|$	Algorithm: steps			
195	$P23$	12	H8	P3c		
196	$F23$	48	H8	P3c	FCent	
198	$P2_13$	12	H8	P3c		
199	$I2_13$	24	H8	P3c	ICent	
215	$P\bar{4}3m$	24	H8	P3c	yx	
216	$F\bar{4}3m$	96	H8	P3c	yx	FCent
217	$I\bar{4}3m$	48	H8	P3c	yx	ICent
218	$P\bar{4}3n$	24	H8	P3c	yx	
219	$F\bar{4}3c$	96	H8	P3c	yx	FCent
220	$I\bar{4}3d$	48	H8	P3c	yx	ICent

Symbols as in Table 1, H8 same as 2x2y2z, use the Hermitian relation to reduce the orthorhombic symmetry (§7).

With this notation,

$$F(\mathbf{h}) = \sum_{g\in G} e_{\mathbf{A}}(\mathbf{A}_1^T\mathbf{h}_0, \mathbf{t}_g) e_{\mathbf{A}}(\mathbf{h}_1, \mathbf{t}_g) Y(\mathbf{R}_g^T\mathbf{h}_1).$$

Let us introduce the notation

$$Z(\mathbf{h}_1, \mathbf{t}_g) = e_{\mathbf{A}}(\mathbf{h}_1, \mathbf{t}_g) Y(\mathbf{R}_g^T\mathbf{h}_1).$$

Then,

$$F(\mathbf{h}_1 + \mathbf{A}_1^T\mathbf{h}_0) = \sum_{g\in G} e_{\mathbf{A}}(\mathbf{A}_1^T\mathbf{h}_0, \mathbf{t}_g) Z(\mathbf{h}_1, \mathbf{t}_g). \qquad (27)$$

The above formula shows how to compute the Fourier transform of the unit cell using only $P1$ Fourier transform of the asymmetric unit (Y). This way, one performs FFT on $1/|G|$ of the starting number of points. This is the maximal possible reduction as one cannot use fewer points than there are in the asymmetric unit. Such a symmetry reduction is possible for a large number of space groups.

A reasoning similar to that in paper II, leading to the same final formula (27), has been performed by Bricogne (1993). However, he built it on a more restrictive assumption that $\mathbf{A}$, $\mathbf{A}_0$ and $\mathbf{A}_1$ all commute with $\mathbf{R}_g$ for every $g \in G$. Such a strict assumption is not necessary and, what is more important, it cannot be satisfied for some of the most interesting cases (*e.g.* the $p3$ symmetry, paper I).

APPENDIX *B*
Tables

The algorithms described in this paper (Tables 1 and 2) depend on the prime-factor decomposition of the number of points in the asymmetric unit. For every space group, there is a family of similar algorithms rather than one algorithm, as was the case in papers II and III. Therefore, a recursive-symmetry decomposition symbol, such as yx should be understood as follows: choose the right algorithm from the family of 'diagonal mirror y, x' algorithms, depending on the periodicity of data. We no longer differentiate symbols for symmetry operators that have the same rotational part, for example y, x and $y+\frac{1}{2}, x+\frac{1}{2}$, we denote them both by yx. The notation is explained in more detail in the table footnote. Each row starts with the ITC number and name of the group, followed by the number of symmetry operators (approximately equal to the speed up achieved by using our algorithms). The last columns contain a list of basic algorithms used (see table footnote for symbol definitions).

The authors are grateful to Jan Zelinka for stimulating discussions and to Marek Koenig for help with illustrations and tables. The research was supported by NIH Grant No. 53163.

References

Bricogne, G. (1993). In *International Tables for Crystallography*, Vol. B. Dordrecht: Kluwer Academic Publishers.
Brünger, A. T. (1989). *Acta Cryst.* A**45**, 42–50.
Hahn, Th. (1995). Editor. *International Tables for Crystallography*, Vol. A. Dordrecht: Kluwer Academic Publishers.
Kudlicki, A., Rowicka, M. & Otwinowski, Z. (2004). *Acta Cryst.* A**60**, 146–152.
Pavelčík, F. (2002). *J. Appl. Cryst.* **35**, 513–514.
Rowicka, M., Kudlicki, A. & Otwinowski, Z. (2002). *Acta Cryst.* A**58**, 574–579.
Rowicka, M., Kudlicki, A. & Otwinowski, Z. (2003*a*). *Acta Cryst.* A**59**, 172–182.
Rowicka, M., Kudlicki, A. & Otwinowski, Z. (2003*b*). *Acta Cryst.* A**59**, 183–192.
Rowicka, M., Kudlicki, A., Zelinka, J. & Otwinowski, Z. (2004). *Acta Cryst.* A**60**, 542–549.
Swarztrauber, P. (1986). *Math. Comput.* A**47**, 323–346.
Ten Eyck, L. F. (1973). *Acta Cryst.* A**29**, 183–191.